LUND UNIVERSITY

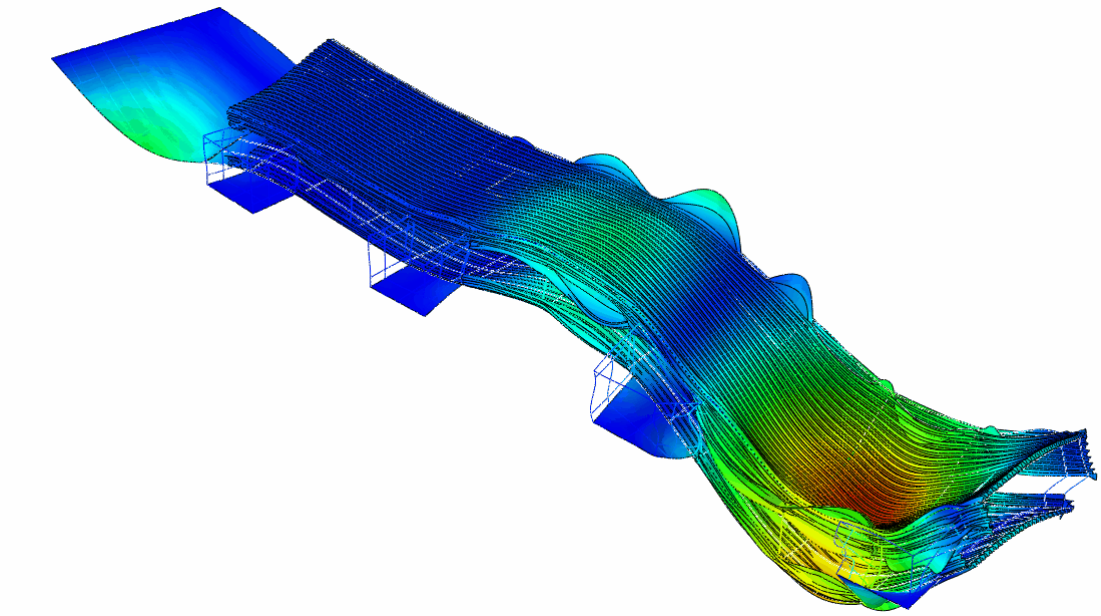

DESIGN OF FOOTBRIDGES SUBJECTED TO DYNAMIC LOADING

PONTUS BRYNK

Structural Mechanics

Masters Dissertation

DEPARTMENT OF CONSTRUCTION SCIENCES
DIVISION OF STRUCTURAL MECHANICS

ISRN LUTVDG/TVSM--22/5260--SE (1-82) | ISSN 0281-6679
MASTER'S DISSERTATION

DESIGN OF FOOTBRIDGES SUBJECTED TO DYNAMIC LOADING

PONTUS BRYNK

Supervisors: Professor **KENT PERSSON**, Division of Structural Mechanics, LTH
together with **PONTUS KARLSSON** and **KENT KEMPENGREN**, AFRY.
Assistant Supervisor: Dr **OLA FLODÉN**, Division of Structural Mechanics, LTH.
Examiner: Associate Professor **PETER PERSSON**, Division of Structural Mechanics, LTH.

Printed by V-husets tryckeri LTH, Lund, Sweden, August 2022 *(Pl)*.

For information, address:
Division of Structural Mechanics,
Faculty of Engineering LTH, Lund University, Box 118, SE-221 00 Lund, Sweden.
Homepage: www.byggmek.lth.se

Abstract

Modern design of steel pedestrian bridges often results in relatively light constructions with low natural frequencies were there is a considerable risk of resonance to occur from loads due to pedestrians. To resolve the problem a common solution is to increase dimensions of load bearing elements, resulting in greatly oversized elements with increasing costs and have substantial environmental impact.

In this rapport it is concluded that oversized dimensions of primary load bearing elements can be avoided with regard to dynamic requirements by implementing a detailed FE-model to evaluate the dynamic response.

This conclusion is found from modeling an existing bridge were the FE-model was calibrated to measurements of the constructed bridge in order to create a realistic model. The dynamic response was evaluated according to SETRA and compared to the outcome when reducing the size of load bearing elements, both models also fulfilling the dynamic requirements according to Eurocode.

The effect of individual parameters in the FE-model on the dynamic response is also investigated to provide guidelines on how to build an accurate model.

Contents

1 Introduction

This chapter provides a background to the subject and descriptions of aim and objectives of the thesis, together with limitations and research questions to be answered in the report. It also presents an outline to help navigating.

1.1 Background

In design of modern pedestrian bridges, it is possible to achieve a slender construction regarding requirements in Ultimate Limit State (ULS). This results in a construction with low natural frequencies, sensitive to vibrations where the dynamic comfort criteria in Serviceability Limit State (SLS) will be critical for the final design.

According to Eurocode the dynamic comfort criteria should be decided as the highest acceptable acceleration of the superstructure. Acceptable acceleration may vary and is to be decided by the developer within each individual project in assistance with recommendations found in respective national annex. The Eurocode specifies that comfort criteria should be verified if the natural frequencies is below 5 Hz in vertical direction and 2,5 Hz in the horizontal direction [1]. The formulation implicates that it is not a requirement to consider the dynamic effect in design of pedestrian bridges and if the first natural frequency are above 5 Hz the accelerations does not need to be verified.

Without requirement to verify the dynamic response there is neither any guidelines on how to conduct a dynamic analysis. A common method adopted is according to the technical guide of "Assessment of vibrational behaviour of footbridges under pedestrian loading" developed by Service d'études techniques des routes et autoroutes (Sètra) a technical department within the French Ministry of Transport and Infrastructure [2]. Sètra provides a guideline on how to apply loading based on mode shapes, natural frequencies, classification and comfort criteria. The most critical step in the analysis is calculation of mode shapes and natural frequencies. The comfort criteria and classification is decided by the developer based on location and usage. For simpler structures mode shapes and natural frequencies can be obtained by hand calculations. More complex structures require use of numeric analysis such as the finite element (FE) Method.

The dynamic response of a FE-model can be highly sensitive and dependent on a variety of parameters who's individual effect on the model is not necessarily intuitive to predict. It has been shown that non load-bearing elements such as railing influences mode shapes and thereby the dynamic behaviour of pedestrian bridges [3]. In a complicated structure it is therefore not evident what to include in creating an efficient and accurate model. Consequently, the outcome from a dynamic analysis using a FE-software, without guidelines and requirements that describes what to include in the FE-model will be highly depending on the previous experience of the engineer.

Natural frequencies and mode shapes mainly depend on the relationship between mass and stiffness while accelerations also depend on damping and loading. [4]. To avoid the need to verify accelerations a common solution is to raise the natural frequencies by increasing the structural stiffness through enlarged dimensions of main load-bearing elements. The subsequent consequence of enlarged dimensions is a simultaneous increase of mass, resulting in an inefficient solution due to low structural utilization in ULS. The outcome of this solution result in an increased financial and environmental impact. Alternative solutions can be to increase stiffness by alteration of the load-bearing structure or decreasing accelerations through installation of mass- or viscous dampers. Neither solution might be acceptable due to the requirement of change in aesthetics or increased overhead costs.

1.2 Aim and Objective

Aim
The aim of the work is to reduce considered cost and environmental impact by eliminating the need of oversized load-bearing elements in construction of steel pedestrian bridges. The aim is to be achieved by give guidelines to develop more accurate and efficient dynamic FE-model for dynamic analysis.

Objectives
The main objective is to determine how different modelling choices influence the dynamic behaviour of the FE-model by conducting a parametric study of a model for an existing bridge, calibrated against measurements of the constructed bridge. With a realistic model, the dynamic response will be evaluated according to current standards to verify the dynamic requirements. Alternative models will also be evaluated against current standards to demonstrate that a more efficient design is possible with regard to dynamic criteria.

1.3 Questioning

To achieve the objectives the report will answer the following questions:

- ➢ Is it possible to create a realistic numeric model to draw conclusions of the influence of individual parameters?
- ➢ Which parameters will have the largest effect on the dynamic behaviour of the numeric model?
- ➢ How does primary load bearing elements affect the dynamic evaluation compared to criteria in Eurocode?
- ➢ How does secondary load bearing elements affect the dynamic evaluation compared to criteria in Eurocode?

1.4 Limitations

The rapport will exclusively focus on:

- ➢ Superstructure of lightweight steel pedestrian bridges.
- ➢ Finite element modelling of a complicated structure.
- ➢ Design choices when creating the numeric model.
- ➢ Vertical accelerations.
- ➢ A single evaluation method for assessment of disturbing vibrations.

1.5 Outline of report

Each chapter begins with a short description of the chapter content to aid navigating.

The rapport is structured to initially introduce the reader to the thesis by providing a background and objective together with the long term aim and limitations in the **Introduction**.

The approach to obtain results answering the questions from the introduction is described in the **Methodology** by providing an overview of the general work process and structure.

To facilitate the reading and help following the rapport a summary of fundamental dynamic theory and evaluation methods are presented in the **Theory** and **Evaluation methods and standards**.

The steel pedestrian bridge studied is presented in **Studied bridge - Skyttelbron** with corresponding numeric model in **FE-model**.

The dynamic behaviour of Skyttelbron are shown in **Numeric studies and results** with conclusions followed in the **Discussion**.

The reader is presumed to possess elementary knowledge of finite element modeling and dynamic analysis including standards and evaluation methods.

2 Structural Dynamics

In this chapter some fundamentals of structural dynamics are presented that will be helpful to understand the content of this report. For further information on the Finite Element method and Abaqus, the reader is referred to *Introduction to the Finite Element Method* [5] and *Abaqus/CAE* [6].

2.1 Multi Degrees Of Freedom System

The generalised equation of motion describing the equilibrium of a Multi Degrees Of Freedom System (MDOF) is presented on matrix format in Equation 2.1, the equation of motion [4]. **M, C** and **K** are the mass-, damping- and stiffness-matrices representing the properties of the system where **ü, u̇** and **p** are vectors describing the location, motion and force acting on each degree of freedom in the system as a function of time.

$$\mathbf{M}\ddot{\mathbf{u}}(t) + \mathbf{C}\dot{\mathbf{u}}(t) + \mathbf{K}\mathbf{u}(t) = \mathbf{P}(t) \tag{2.1}$$

2.1.1 Natural frequencies

By neglecting damping and force in Equation 2.1 natural frequencies and mode shapes can be obtained through solving for free vibration system. The solution to results in the homogeneous system of equation described by Equation 2.2 which constitutes an eigenvalue problem that yields N natural frequencies ω_n with corresponding mode shape ϕ_n.

$$\begin{aligned} (\mathbf{K} - \omega^2\mathbf{M})\phi = 0 \quad &\longrightarrow \quad det(\mathbf{K} - \omega^2\mathbf{M}) = 0 \\ \omega_n = [\omega_1, \omega_2, \cdots, \omega_N] \quad &\text{are eigenvalues} \\ \phi_n = [\phi_1, \phi_2, \cdots, \phi_N] \quad &\text{are eigenvectors } [N, 1] \end{aligned} \tag{2.2}$$

2.2 Damping

Damping is representing energy losses in the system. The relation between damped and un-damped natural frequencies are described by Equation 2.3 [4] were damping have a negligible impact on the natural frequencies for damping values $\zeta < 20\%$.

$$\omega_{n,D} = \omega_n \sqrt{1 - \zeta_n^2} \quad \longrightarrow \quad \omega_{n,D} \approx \omega_n \tag{2.3}$$

$$\text{when} \quad \zeta \quad \text{is small} \quad \text{and} \quad \zeta_n = \frac{c_n}{2m\omega_n}$$

Dynamic Amplification Factor and resonance
The effect damping have on accelerations can be described by the Dynamic Amplification Factor (DAF) in Equation 2.4. The DAF is a scaling factor for the accelerations, depending on the damping ζ and loading frequency ω in relation to natural frequencies ω_n. Resonance is when accelerations increase drastically, described by the DAF, as the loading frequency approaches the natural frequency, plotted for a variation of damping values in Figure 2.1

$$R_d = \frac{1}{\sqrt{(1 - r^2)^2 + (2\zeta r)^2}} \tag{2.4}$$

$$\text{were} \quad r = \frac{\omega}{\omega_n}$$

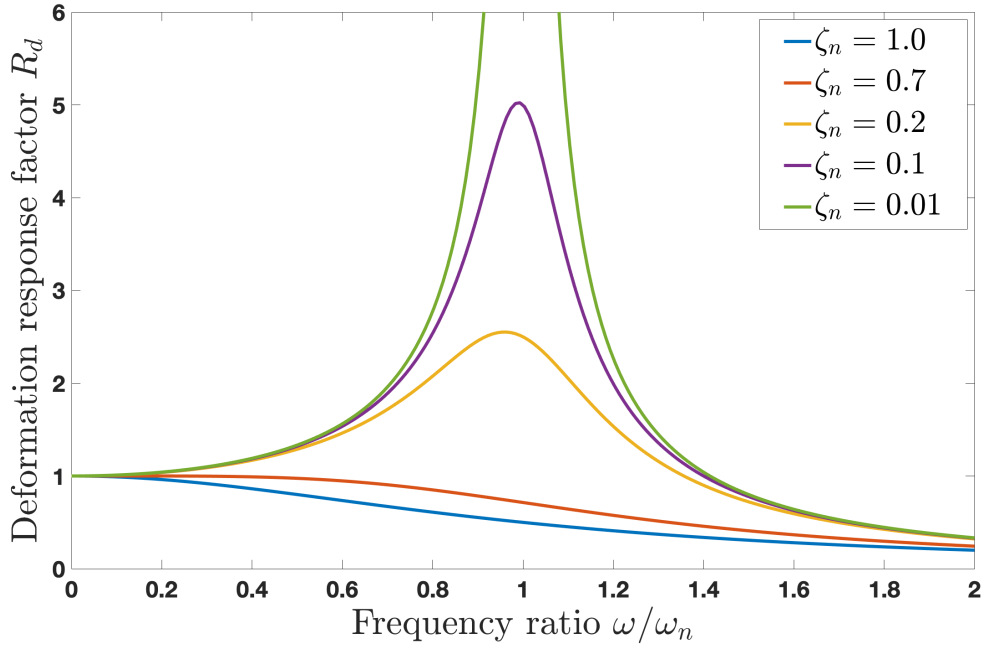

Figure 2.1: DAF plotted for loading frequencies around the natural frequency, illustration inspired by Chopra K. Anil. [4].

2.2.1 Modal analysis

By using a modal expansion, the displacement vector $\mathbf{u}$ can be expressed with the eigenvectors ϕ used as base vectors shown in Equation 2.5 [4].

$$\mathbf{u}(t) = \sum_{i=1}^{N} \phi_i q_i(t) = \Phi \mathbf{q}(t) \tag{2.5}$$

where
$$\begin{aligned} q_i(t) &= A_i cos(\omega_i t) + B_i sin(\omega_i t) \\ \mathbf{q}(t) &= [q_1(t), q_2(t), \cdots, q_N(t)] \\ \Phi &= [\phi_1, \phi_2, \cdots, \phi_N] \\ \phi_i &= [Nx1] \end{aligned}$$

Modal truncation
If the loading does not trigger higher modes, a accurate result can be obtained using a truncated system where only $J < N$ modes contribute to the displacement, described by Equation 2.6. The truncated system can there by reduce the amount of calculation drastically at a very low cost.

$$\mathbf{u}(t) = \sum_{i=1}^{J} \phi_i q_i(t) \tag{2.6}$$

2.3 Frequency Response Function

The Frequency Response Function (FRF) is a transfer function that translates an applied force into a structural response, described by Equation 2.7 and illustrated in Figure 2.2.

The FRF of FE-model is used to predict the structural response to a given loading, where the FRF can be expressed analytical by using modal analysis. Conducting acceleration measurements the FRF can be obtained for the constructed structure and used to validate the FE-model.

The response can be given in form of displacement, velocity or acceleration but is always, by definition, in relation to a normalized load. For practical reasons the FRF is most commonly chosen for the frequency domain, but can also be given for the time domain, where ω in Equation 2.7 is exchanged for t.

$$H(\omega) = \frac{u(\omega)}{F(\omega)} \tag{2.7}$$

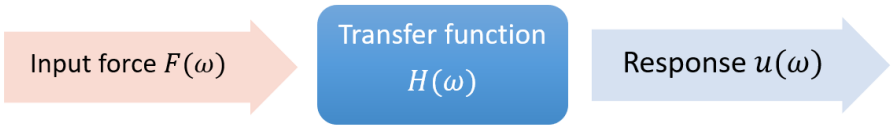

Figure 2.2: Illustrates how the FRF translates a force input into a structural response.

3 Methodology

This chapter describes steps taken in the work process to obtain grounds for discussions and conclusions presented in the end of the rapport. To answer the questions in 1.3 an existing bridge, Skyttelbron described in Chapter 5 were modeled using FE-software. The FE-model were used for a parametric study and evaluation of the dynamic response with regard to requirements in Eurocode.

3.1 Work Process

The work process can be divided into 3 main phases, partly overlapping, consisting of a literature review to determine prerequisites followed by FE-modelling and finally evaluation of results, summed up in a rapport.

An overview of the general work-process is visualized in Figure 3.1 were each main phase is further divided in to smaller steps described in respective sub-chapter.

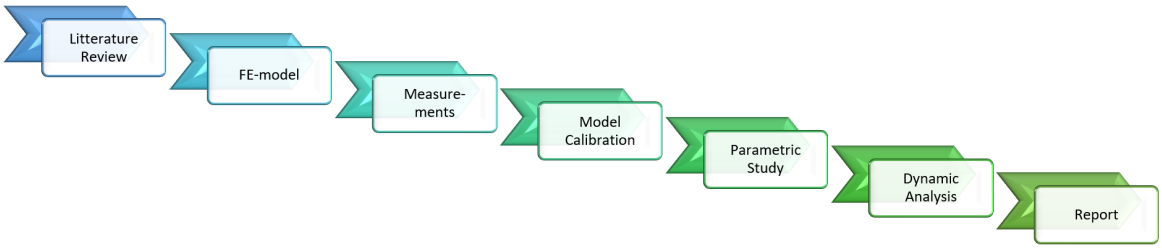

Figure 3.1: Flow chart of the general work process.

3.1.1 Literature Review

Initially a literature review was conducted to identify relevant information on dynamic design of pedestrian bridges, relevant standards and dynamic requirements.

The literature review resulted in a the choice of dynamic evaluation method described in 4.2, dynamic requirements according to Eurocode and the conclusion that there have not been much research made on the specific topic of how to model more complex structures using FE-modelling with regard to the dynamic behaviour.

3.1.2 FE-Model

An FE-model of an existing bridge was created according to construction drawings described in Chapter 5 in an iterative modelling process while evaluating the dynamic behaviour of the model by assessing mode shapes.

3.1.3 Measurements

The dynamic behaviour of the constructed bridge was obtained by measuring the acceleration response from an impulse excitation on the bridge, described in Chapter 6.

3.1.4 Model Calibration

To generate reliable results and answering the questions in 1.3 it is essential to create a realistic FE-model reflecting the dynamic response of the real structure. Model properties of the FE-model were therefore adjusted for the purpose of obtaining a dynamic response that was closer to that of the actual bridge. This created a model used as a reference model, described in Chapter 7.

3.1.5 Parametric Study

The parametric study was conducted by altering individual parameters of the reference model in steps. The dynamic response was compared with the reference model to evaluate the effect of altered parameter. Investigated parameters were stiffness and mass with alterations as shown below with original configuration of ***the reference model marked in bold***.

- **Stiffness**
  - Facade - Corrugated steel: thickness of the reference model ***1***, 2 and 5 mm
  - Deck: thickness ***10***, 15 and 25 mm
  - Stabilizing beams: ***rotation free joints***, stiffened joints (locked rotation), increased E-modulus and removed from the model.
- **Mass**
  - Quantity - Mass of installations: ***100%***, 0%, 150% and 200%
  - Distribution: ***line load***, point mass and uniform load

3.1.6 Dynamic Evaluation

Dynamic properties were evaluated based on natural frequencies causing resonance in the deck and corresponding maximum accelerations from pedestrian loading, modeled according to Sètra as described in Chapter 4.2.

In design of pedestrian bridges, natural frequencies are of primary interest to avoid resonance from pedestrians walking which have a frequencies in the interval between 1-3 Hz [2]. Natural frequencies of an FE-model are found by an eigenvalue analysis as described in Chapter 2.

Accelerations are only of interest to evaluate when there is a considerable risk for resonance to occur. Accelerations are strongly dependent on load application and frequency, but also damping and need to be evaluated in relation to a chosen method. This is because acceleration criteria are determined in relation to procedures of that specific method. Meaning that results from one evaluation method not necessary can be compared to general acceleration criteria.

In design of pedestrian bridges accelerations are of secondary interest, only to consider when there is a considerable risk for resonance to occur. Accelerations are strongly dependent on load application and frequency, but also damping and need to be evaluated in relation to the chosen method. This because acceleration criteria are determined in relation to procedures of that specific method, meaning results from one evaluation method not necessary can be compared to general acceleration criteria.

Dynamic properties have been evaluated for 3 models, described shortly below and in detail in Chapter 7.

Model 1 The reference model calibrated to follow the behaviour of the constructed bridge. Dynamic properties of this model, used as reference, are evaluated to confirm fulfillment of dynamic design criteria for the constructed bridge.

Model 2 In this model, the primary load bearing elements are reduced in order to determine if the bridge could have been constructed with a more efficient design, regarding dynamic design criteria. Dynamic properties are also for this model evaluated to confirm its fulfillment of dynamic design criteria.

Model 3 In this model the corrugated steel, representing the facade, is removed to determine how it effects the outcome of the dynamic analysis regarding criteria set in Eurocode.

3.1.7 Report

Writing the report includes to provide a problem description together with aim and objective of the thesis to motivate the importance of the work. It also gives a clear description of the work procedure to obtain reliable results used as ground for discussion and conclusions to fulfill set out objective.

3.2 FE-modelling approach

The FE-model is built to mimic real conditions of the constructed bridge where elements, constraints, material etc. are based on the construction drawings. The objective with the initial model, **Model 1**, is to include all known parts of the bridge in order for the parametric study to conclude the effect on individual parts and determine which ones that are necessary to include when creating an FE-model to be used for assessing vibration criteria.

Modelling options that were impossible to determine based on the construction drawings or other information known prior to construction were progressively tested and evaluated during the modelling phase. The modelling procedure is described shortly below.

- **Boundary conditions:**
  Known boundary conditions of supports are modelled according to construction drawings while others, based on modelling choices, were gradually tested and evaluated during the modelling process. These boundary conditions were continuously moved further away from the points of interest by extending the model, adding more sections. This was done to ensure that boundary conditions do not have a negative impact on the dynamic behaviour.

- **Secondary elements:**
  All secondary elements were included in **Model 1**.

- **Mass quantity:**
  Modeled elements were assumed to have a mass based on respective material and profiles. Non-structural mass of elements excluded from the model is to the extent of knowledge of material and quantity, otherwise estimated and later adjusted in the model calibration.

- **Mass distribution:**
  Masses are modeled with an as realistic distribution as possible. The outcome of different alternatives of the distribution of non-structural mass was, however, tested during the modeling process.

3.3 Dynamic analysis by FE-modeling

The FE-software Abaqus was used to create all FE-models and for conducting all dynamic analyses, [6].

3.3.1 Eigenvalue analysis

Natural frequencies and modes were determined through an eigenvalue analysis in the frequency interval of 0-40 Hz using a SIM base linear procedure and Lanczos eigensolver. The range of the frequency interval was chosen in order to obtain valid accelerations for relevant loading frequencies when using the modes in a truncated modal analysis.

3.3.2 Frequency Sweep

Peak accelerations are obtained by conducting a frequency sweep using Steady State Dynamic modal analysis (SSDm). The load frequency was linearly subdivided into 20 points between natural frequencies from the eigenvalue analysis, and a bias of 3 to smothering the plotted curves close to resonance frequencies. The frequency interval is chosen to 0-15 Hz with 4.5% modal damping in order to compare the FE-models response with measurements of the constructed bridge.

3.3.3 Finite elements and problem size

The FE-element model of Skyttelbron was built using beam- and shell elements named B31 and S4R in Abaqus. The elements are described further below with final mesh size shown in Table 3.1

Shell S4R: 4-node general-purpose shell with 6 degrees of freedom (DOF) per node, reduced integration with hourglass control. Simpsons thickness integration rule using 5 integration points. Element size are set to 0.1 m^2

Beam B31: 2-node linear 3D-beam with 6-DOFs and element size of 0.1 m.

Table 3.1: Mesh size in number of elements, nodes and DOFs.

Elements	Nodes	DOFs
192166	210549	1175082

4 Evaluation methods and Standards

This chapter present dynamic design criteria found in Eurocode and the Sétra method to evaluate vibration criteria in SLS.

4.1 Eurocode

4.1.1 Functional requirements

Functional requirements in serviceability limit state for pedestrian steel bridges are formulated in Eurocode 3: Design of steel structures - Part 2 Steel Bridges states in chapter 7.9 of SS-EN 1993-2:2006 functional requirements.

(1) Pedestrian bridges with to high oscillations, which can result in reduced comfort levels, should be resolved to minimize such by designing the bridge with appropriate natural frequencies or equip it with appropriate damping devices.

4.1.2 Traffic loading

Dynamic models of pedestrian loading is described in Eurocode 1: Actions on structures – Part 2: Traffic loads on bridges in chapter 5.2 of SS-EN 1991-2 dynamic models of pedestrian loading.

(1) Depending on the dynamic properties of the bridge structure, with respect to natural frequencies in respective direction, the design of the main structure of the bridge should be design assistance of an appropriate structural model.

(2) Loading from pedestrians were loading frequency matches any of the bridges natural frequencies might give raise to resonance and have to be considered when verifying oscillations in the serviceability limit state.

-in the vertical direction this reference to a frequency range between 1 and 3 Hz.

(3) Applicable dynamic models, modeling pedestrians and criteria regarding comfort should be decided.

4.1.3 Comfort Criteria

Comfort criteria for vibrations in pedestrian bridges is described in Eurocode - Basis of structural design SS-EN 1990 chapter A2.4 comfort criteria of pedestrians (in serviceability limit state).

(1) Comfort criteria should be decided as the maximum acceleration that can be accepted for each individual part of the superstructure.

Following values concerns recommendation of maximum acceleration for an arbitrary part of the superstructure.

i) 0.7 (m/s^2) for vertical vibrations.

(2) Comfort criteria should be verified for natural frequencies of the superstructure below

- 5 Hz in the vertical direction.

4.2 Vibration evaluation according to SETRA

The generalized method for evaluating acceleration of pedestrian bridges according to Service d'études techniques des routes et autoroutes, (Sétra) with regard to vertical accelerations are presented here.

Footbridges; Assessment of vibrational behaviour of footbridges under pedestrian loading is a technical guide developed by Sétra, a technical department within the French Ministry of Transport and Infrastructure. An overview of the method is displayed by a flow chart in Figure 4.1

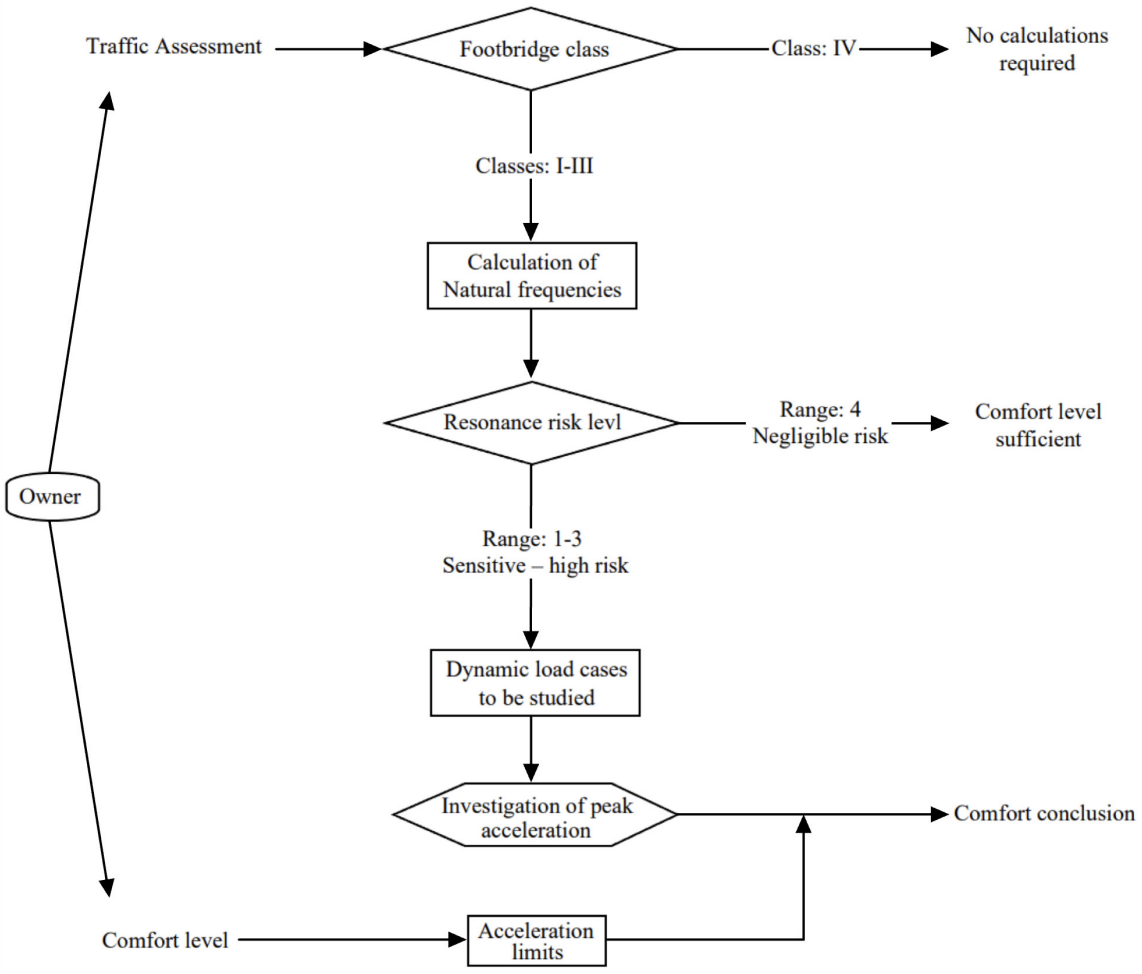

Figure 4.1: Flowchart over the Sétra method. Illustration based on Sétra [2].

4.2.1 Sétra methodology

1. Traffic assessment
Prediction of future traffic is estimated in a traffic assessment based on location and intended use of the bridge, resulting in a classification in one of class I-IV. The bridge class is relating to crowd density and relevant load cases to analyze if natural frequencies subside 5 Hz.

Classification requirements:

Class I: urban footbridge linking up high pedestrian density areas (for instance, nearby presence of a rail or underground station) or that is frequently used by dense crowds (demonstrations, tourists, etc.), subjected to very heavy traffic.

Class II: urban footbridge linking up populated areas, subjected to heavy traffic and that may occasionally be loaded throughout its bearing area.

Class III: footbridge for standard use, that may occasionally be crossed by large groups of people but that will never be loaded throughout its bearing area.

Class IV: seldom used footbridge, built to link sparsely populated areas or to ensure continuity of the pedestrian footpath in motorway or express lane areas.

2. Calculations of natural freqeuencies
Natural frequencies are to be determined for 2 mass assumptions:

Empty footbridge: determine natural frequencies for an empty footbridge, without any extra mass.

Pedestrian loaded: determine natural frequencies for an footbridge with a fully loaded bearing area of pedestrians corresponding to 70 kg/m^2.

3. Resonance Risk level
Risk of resonance is based walking and running frequencies in relation to the bridge's natural frequencies. Ranges are illustrated in Figure 4.2

Range 1: maximum risk of resonance.
Frequencies in the interval between 1.7-2.1 Hz.

Range 2: medium risk of resonance.
Frequencies in the interval between 1.0-1.7 and 2.1-2.6 Hz.

Range 3: low risk of resonance for standard loading situations.
Frequencies in the interval between 2.6-5.0 Hz.

Range 4: negligible risk of resonance. No further calculations required.
Frequencies <1.0 and >5.0 Hz.

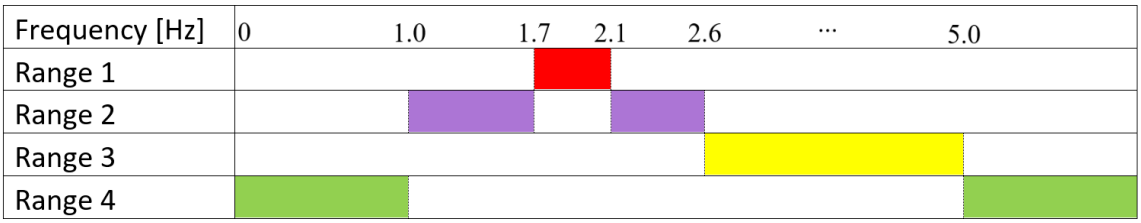

Figure 4.2: Frequency ranges corresponding to respective Range describes above. Illustration based on Sétra [2].

4. Dynamic load-cases
Load-cases has been constructed by Sétra for each frequency range to simplify the effect a variation in load magnitude and risk for resonance. The load is to be applied in form of the mode shape corresponding to the natural frequency being evaluated, example of loading is shown in Figure 4.4 and critical damping in Table 4.1.

Load Case 1: are designed for sparse and dense crowd corresponding to bridges in class II and III in frequency range 1.0-2.6 Hz to be applied according to Equation 4.1.

Load Case 2: are designed for a very dense crowd corresponding to bridge class I in frequency range 1.0-2.6 Hz to be applied according to Equation 4.2.

Load Case 3: are designed considering the second harmonic, caused by walking pedestrians, on average found at twice the frequency of the first harmonic. This load case is only relevant for bridges in class I and II to be applied according to Equation 4.3.

$$p_v(t) = d \cdot 280 \cdot cos(2\pi \cdot f_i \cdot t) \cdot 10.8\sqrt{\varepsilon/n} \cdot \psi \tag{4.1}$$

$$p_v(t) = 1.0 \cdot 280 \cdot cos(2\pi \cdot f_i \cdot t) \cdot 1.85\sqrt{1/n} \cdot \psi \tag{4.2}$$

$$p_v(t) = 1.0 \cdot 70 \cdot cos(2\pi \cdot f_i \cdot t) \cdot 1.85\sqrt{1/n} \cdot \psi \tag{4.3}$$

where Equation 4.1-4.3 can be expressed as:

$$p_v(t) = p_{0,j} \cdot cos(2\pi \cdot f_i \cdot t) \cdot \psi \tag{4.4}$$

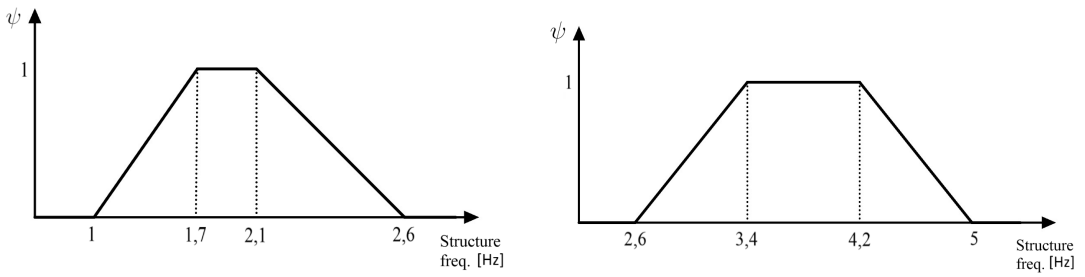

(a) Frequency interval for the first harmonic. **(b)** Frequency interval for the secon harmonic.

Figure 4.3: Reduction factor ψ for frequency intervall of first and second harmonic. Illustration based on Sétra [2].

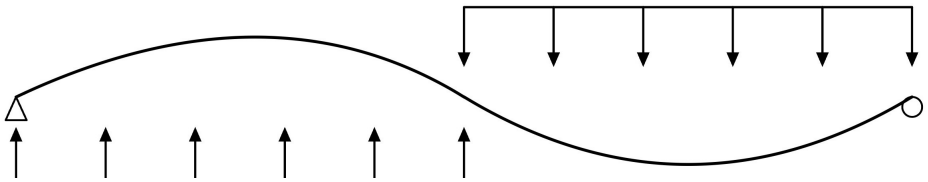

Figure 4.4: Example of loading application in form of mode shape. Illustration based on Sétra [2].

Table 4.1: Critical damping ratio to be taken into account, according to Sétra. Critical damping may be taken as a weighted average corresponding to the material ratio.

Type	Critical damping ratio
Reinforced concrete	1.3%
Pre-stressed concrete	1.0%
Mixed	0.6%
Steel	0.4%
Timber	1.0%

5. Acceleration limits

Evaluating comfort criteria, peak accelerations is divided into 4 ranges corresponding to comfort class described below and shown in Figure 4.5

- **Range 1**: acc<0.5 m/s^2 results in maximum comfort level.
- **Range 2**: acc<1.0 m/s^2 results in medium comfort level.
- **Range 3**: acc<2.5 m/s^2 results in minimum comfort level.
- **Range 4**: acc>2.5 m/s^2 is not acceptable for any bridge.

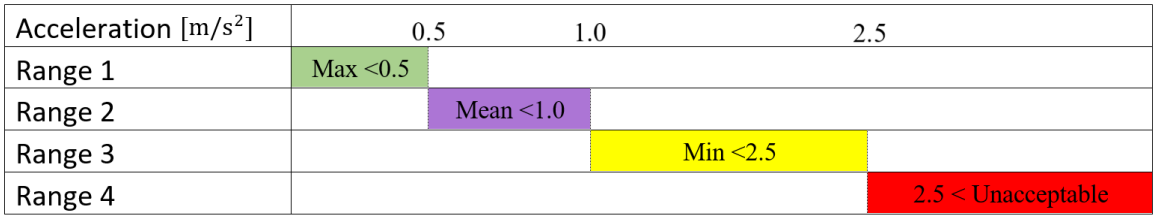

Figure 4.5: Acceleration interval corresponding to respective comfort range. Illustration based on Sétra [2].

4.2.2 Summary

Evaluate natural frequencies of the bridge.

Chose load case and crowd density from Table 4.2 for natural frequencies <5 Hz corresponding to the bridge classification in step 1, traffic assessment.

Calculate the load according to Equation 4.1-4.3 and apply the load in form of the mode shape corresponding to the natural frequency being evaluated.

Apply critical damping according to Table 4.1 and calculate peak accelerations.

Compare accelerations to comfort levels in Table 4.5.

Table 4.2: Overview of the Sétra method.

Class	Crowd density [pedestrians/m^2]	Frequency range [Hz]	
		1.0-2.6	2.6-5.0
I	1.0	Case 2	Case 3
II	0.8	Case 1	Case 3
III	0.5	Case 1	Case 3
IV	No calculations requiered		

5 Studied bridge - Skyttelbron

This chapter presents the design of the studied bridge, Skyttelbron located at Lund Centeral station and shown in Figure 5.1. The chapter starts with a summary and general description to provide a quick overview. Details are in the following further described.

Figure 5.1: Skyttelbron, located at Lund central station.

5.1 Summary

The 66 m long, approximate 300-ton heavy pedestrian bridge, Skyttelbron consists of four spans between 13.2-16.4 m, primarily built with HEA-500 and HEA-280 steel beams. A overview of the structure can be seen in Figure 5.2 were the forth span consists of a ramp, connecting the bridge to the west side of Lund. The superstructure is constructed with ridged frames places with various distances, connected to the floor beams. The deck is made up of three layers, concrete, steel and isolation, and is 7.2 m wide with a total surface area of 504 m^2. Windows and corrugated steel attached to the frame makes up a surface area approximate to 70 and 960 m^2 respectively.

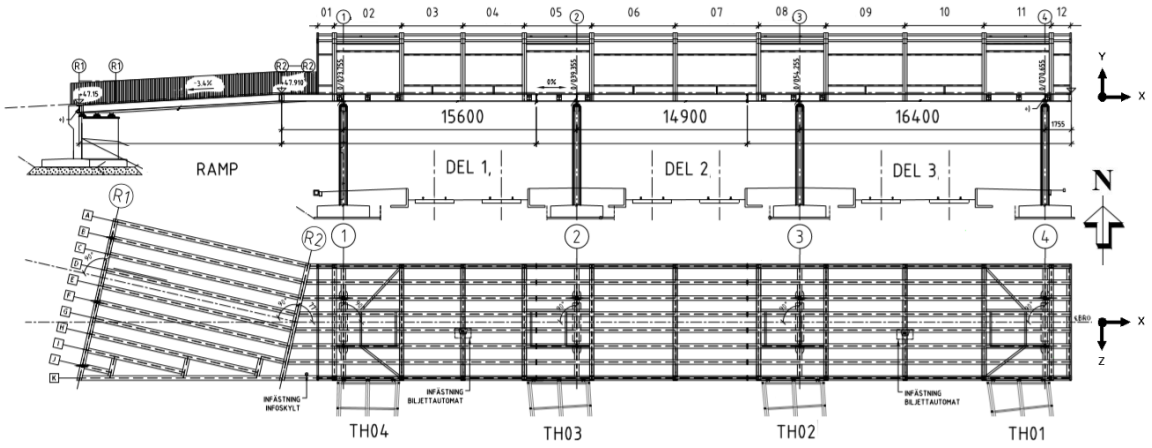

Figure 5.2: Construction drawing of the complete bridge [7].

5.2 General description

Skyttelbron is a 66-meter-long, covered steel- pedestrian bridge connecting the city central and west side of Lund. It allows pedestrians to both cross the railway and to access the train platforms.

The pedestrian bridge is orientated in west-east direction and consists of 4 spans with lengths between 13.2-16.4 m. Span 1-3 will be referred to as the main deck, connected to the ramp. Stairwells to the train platforms are located near each support on the south side of the bridge. Covering, windows and installations are attached to a rigid frame in the superstructure. The frames are connected to the floor beams and makes up a total of 12 sections.

Directions of the bridge will be described by a coordinate system or cardinal direction shown in Figure 5.2. Using the coordinate system as reference, the X- and Y-axis constitutes longitudinal and vertical direction. The Z-axis is oriented in the transverse direction from north-south. Line 1-4 and R1 marks supports while R2 marks the transition between the ramp and first span. The ramp makes up the trapezoid shaped west span of the bridge.

5.2.1 Bridge structure

The bridge is made up of a floor beams, deck, frame and covering. Floor beams and deck is marked in red and while frame and covering is marked in blue, shown in Figure 5.3.

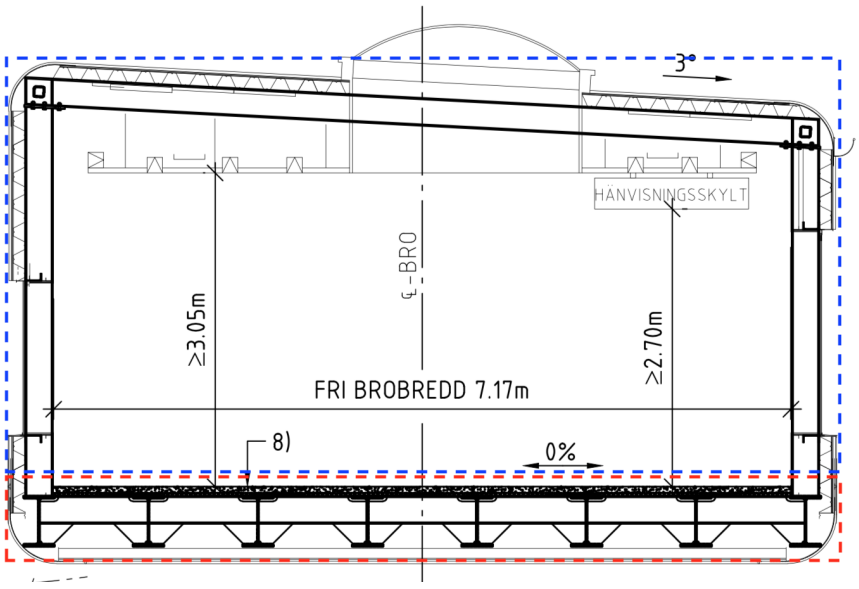

Figure 5.3: Cross section of the bridge, displaying structural elements [7].

Floor beams
The deck is constructed with a rigid cross joint-system of HEA-500 and HEA-280 beam element as primary- and secondary load-bearing element.

Deck
Cross section of the deck is made up three layers. Top layer, the wearing surface, made of concrete is separated from a bottom steel plate by isolating cell-plaster.

Frame
HEA-280 beam element constitutes the rigid frame, connected to the deck. The frames are placed along the deck with various distance aligned with transversal HEA-280 elements making up a total of 12 section. Different height of the columns entails a slight inclination of the roof. End-frames are made of UPE-270 beam elements.

Facade
The facade is made from corrugated steel and windows attached to frame and sides of the superstructure.

5.2.2 Stairwells

The stairwells attached to the south side of the superstructure, connecting the bridge and platform, are built with a concrete- elevator core as primary support shown in Figure 5.4.

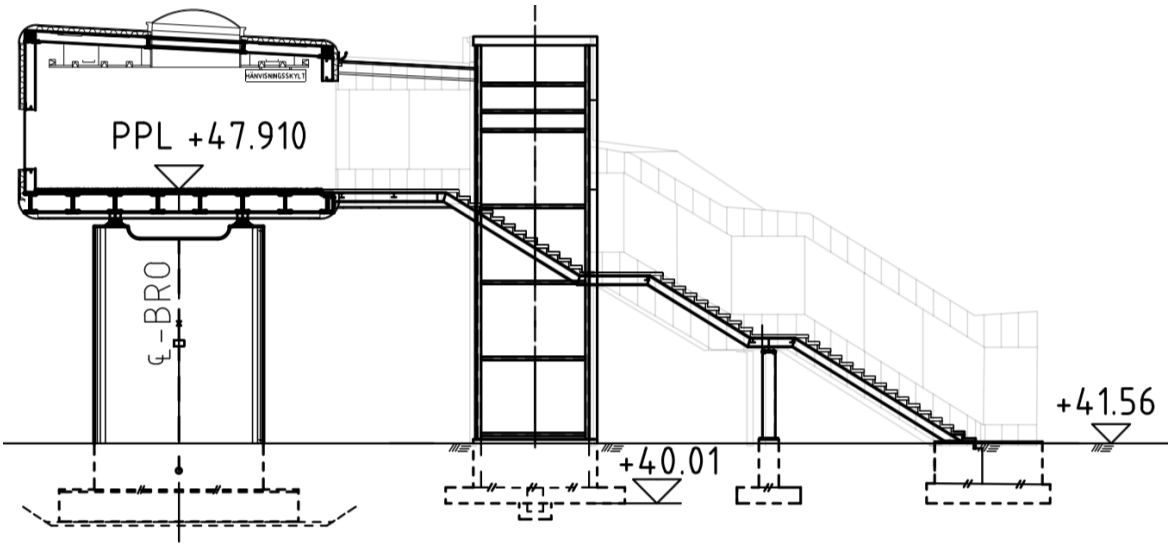

Figure 5.4: Stairwells connected to the bridge [7].

5.3 Main deck

Eight HEA-500 beam element with a cc-distance of 1065 mm, placed in the longitudinal direction constitutes the primary load-bearing elements of the main deck, span 1-3. Primary beam elements, marked A-H, are assembled together from three pieces with a moment stiff, bolted connection shown in Figure 5.5. HEA-280 beams make up secondary load-bearing elements, distributing loads between primary elements in the transverse direction. The transverse HEA-280 elements are welded on to primary beams with distances between 4.1-5.8 m to match frame sections.

Additional HEA-500 beam elements are placed at supports to transfer loads from primary beam element to point C and F connected to the abutment.

The deck is reinforced with HEA-500 beams to transfer loads to the four point-supports placed along beam element C and F.

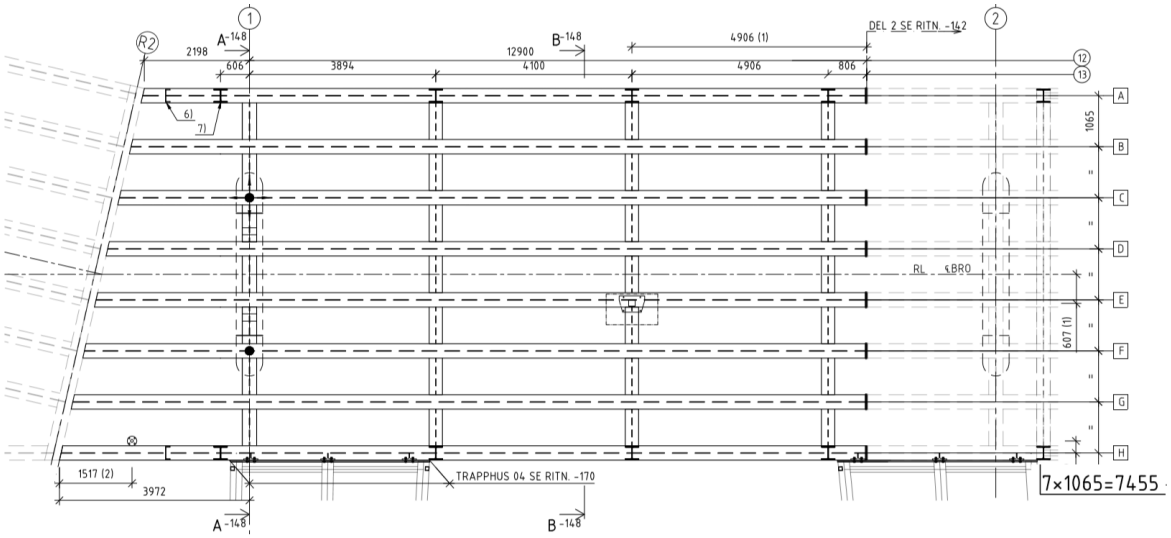

Figure 5.5: Detailed construction drawing of the main deck [7].

5.3.1 Ramp

The ramp constituted the fourth span connecting the main bridge to the west side of Lund, shown in Figure 5.2. It constitutes a 13.2 m long trapezoid shaped span tilted in a 3-degree angle due to a height difference of 760 mm between the abutment and main deck. The structure is similar to the main deck with HEA-500 beams as primary load-bearing elements and end-beams. It is welded together with the main deck at a 13 degrees angle shown in Figure 5.6.

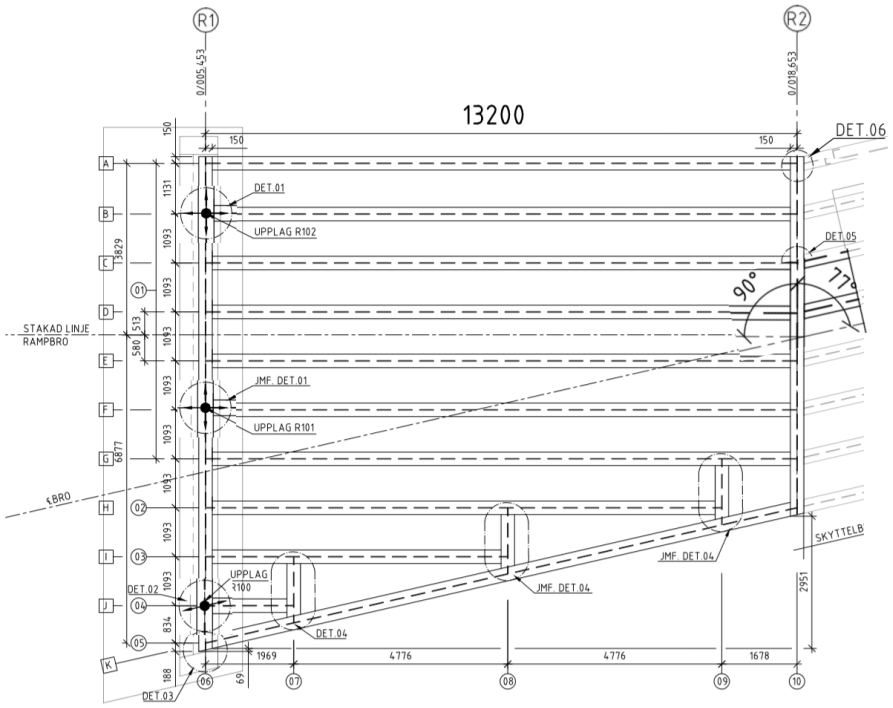

(a) Top view of the ramp.

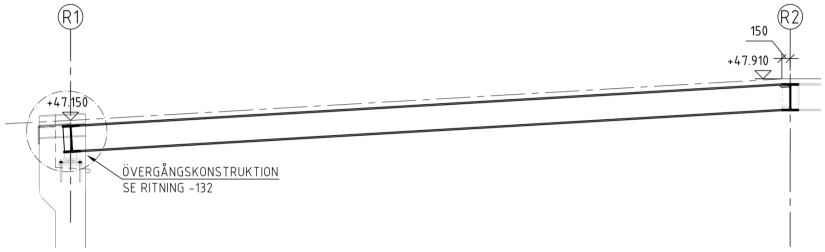

(b) Profile of the ramp.

Figure 5.6: Detailed construction drawing of the ramp [7].

5.3.2 Connections

Primary beam elements - Longitudinal direction
Primary beam elements were assembled together at sight to one continuous beam from three individual pieces with lengths between 15.1-21.7 m. They are joined in span 1 and 2 connected with a bolted connection of 12 bolts in class M24-S10.9 as shown in Figure 5.10.

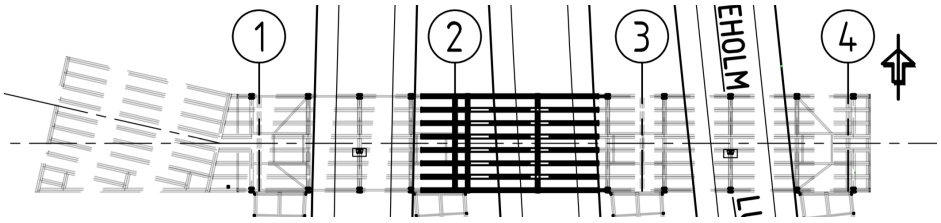

(a) Placement of joint.

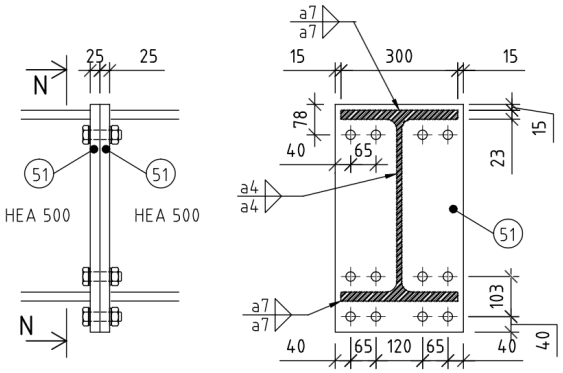

(b) Details of bolted connection.

Figure 5.7: Connection between the longitudinal HEA500 beam members. [7].

Secondary beam elements - Transverse direction
Secondary beams are welded on to the web and flanges of the primary beams were HEA-280 beams are fitted with an extra, 15 mm steel plate shown in Figure 5.8.

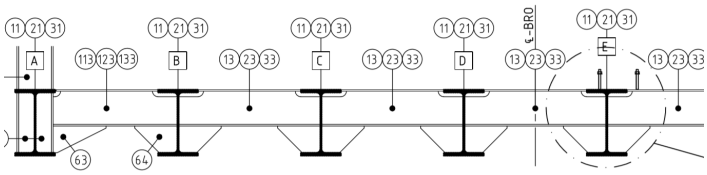

(a) joint between transversal HEA280 and longitudinal HEA500 beams.

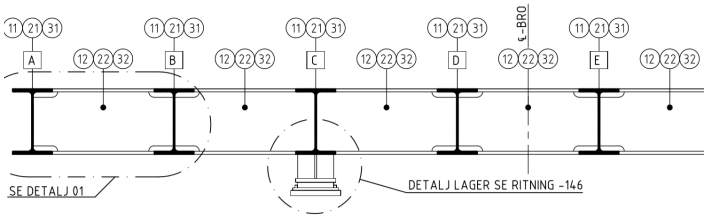

(b) Joint between transversal and longitudinal HEA500 beams.

Figure 5.8: Joints in the cross-joint system of the floor beams [7].

Ramp-Span 1
The ramp connects to the first span by a welded connection were primary load bearing elements are welded on to a common end beam shown in Figure 5.9.

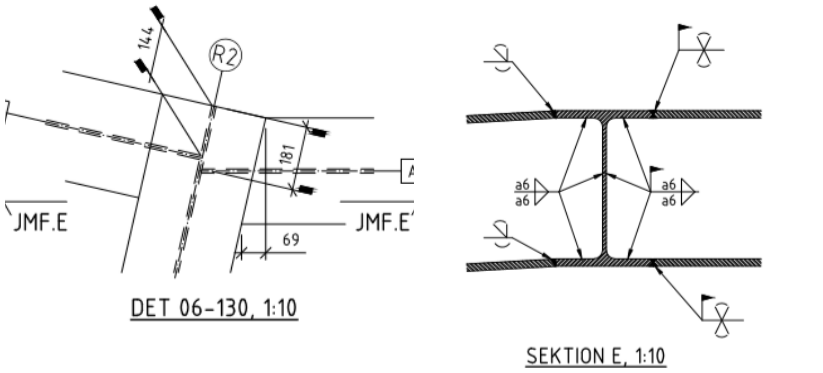

(a) Top side of the connection between ramp and main deck.

(b) Profile of the connection between ramp and main deck.

Figure 5.9: Joint between ramp and main deck [7].

5.3.3 Deck

The cross section of the main deck is 7.17 m wide and have a total surface area of 383 m^2 with a total of 504 m^2 including the ramp. The cross section consists of three layers; steel, isolation and concrete shown in Figure 5.10. The wearing surface is made of 60 mm cast C35/45 concrete. The bottom layer, in connection to the deck, consists of a 10 mm steel walkway-plate. The concrete and steel plate are separated by 30 mm cell plaster, polystyrene (XPS). Interaction between the steel plate and concrete is restricted to pairs of studs placed along primary beam element E in the longitudinal direction.

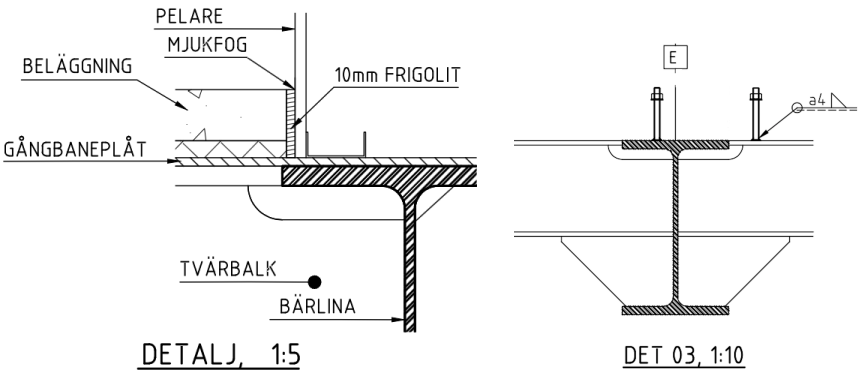

(a) Cross section of the deck.

(b) Connection of studs to the floor beams.

Figure 5.10: Properties of the deck [7].

5.4 Superstructure

HEA-280, column- and beam elements constitutes a rigid frame, bolted together in the corners and connected to the deck by welded joints shown in Figure 5.11. The frames are placed with distances varying between 4.1-5.8 m, making up twelve compartments with a combined length of 50 m. Columns of the frame are 3.8 and 3.6 m resulting in a slight roof inclination of 3 degrees over the 7.5 m span.

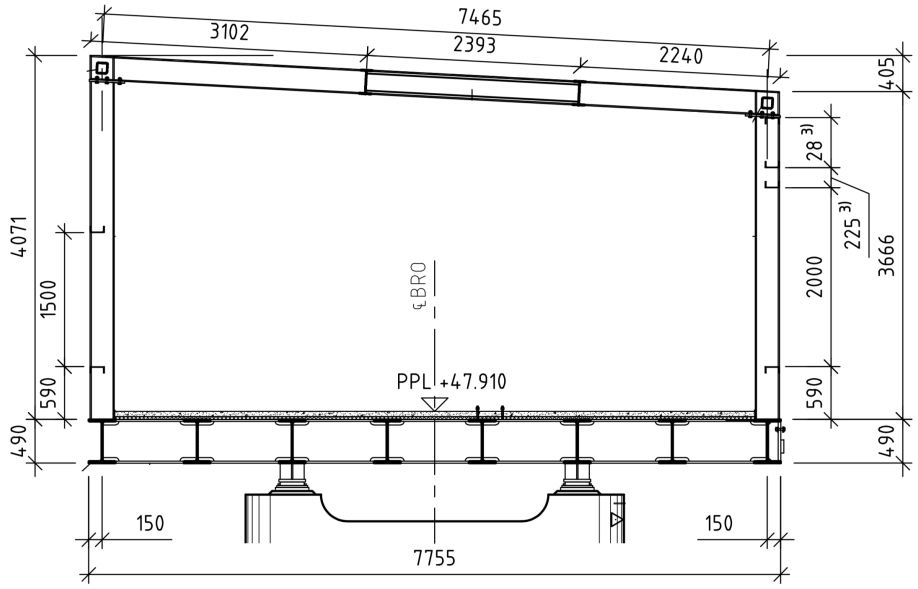

Figure 5.11: The cross section of the bridge [7].

5.4.1 Top section

Frame-sets are connected together in the longitudinal direction by beam elements with a 5 mm thick, 120x120 KKRK-profile (17). The KKRK-elements are connected to the frame in top corners with welded joints (detG). Skylights are installed in 4 places attached to the frame by a configuration of IPE-200 (20A) and IPE-270 (19) beam elements, connected with a bolted connection (detE). The rigid, bolted connection between elements of the frame (detF) is marked in Figure 5.12.

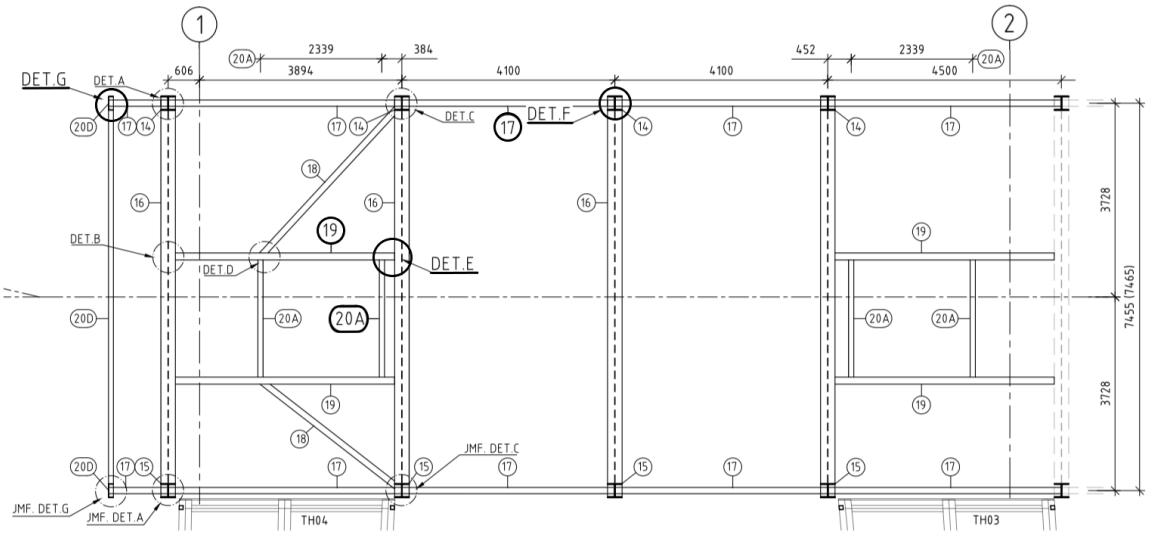

Figure 5.12: Detailed view of the top section of the frame with marked joints [7].

5.4.2 Sides sections

Windows and covering are supported by UPE-160 (20B) beam elements, welded (detJ) against the deck and bolted (detI) to the frame shown in Figure 5.13. Frame set on both ends are made up of UPE-270 (20D).

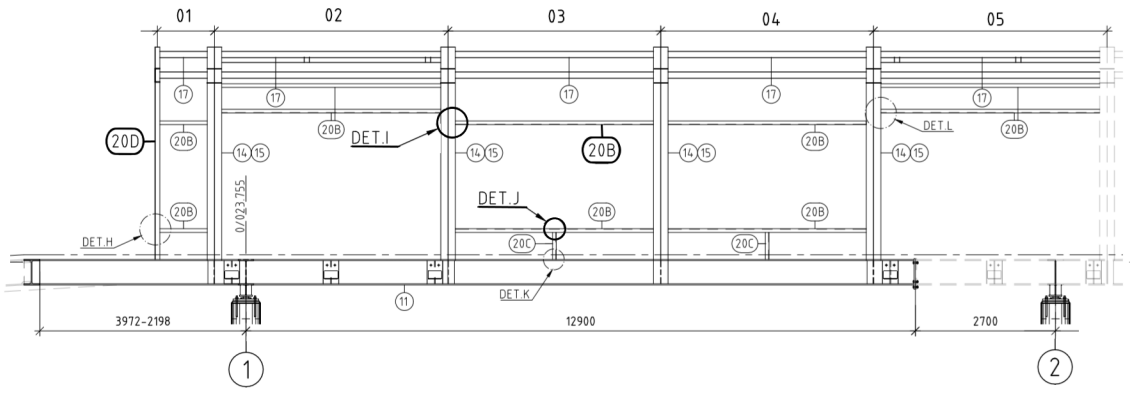

Figure 5.13: Detailed view of the side section of the frame with marked joints [7].

5.4.3 Connections in the superstructure

All joints in the upper superstructure shares a few base designs with some individual differences. Principals of the base design and joints assessed to be of extra importance to FE-model are presented here.

Connections in the top section
Det E: IPE profiles supporting the skylights are bolted on to a steel plate attached to the web and flanges of the transverse HEA-280 beams shown in Figure 5.14a.

Det F: The top of the columns is fitted with an end-plate, welded in place. The end-plate is bolted together with the bottom flange of the beam. The web is braced with two plates, welded in place in line with flanges of the column shown in Figure 5.14b.

Det G: longitudinal KKRK profiles connecting together frame sets, are welded on to the web of the HEA-280 beam elements in the frame corners shown in Figure 5.14c.

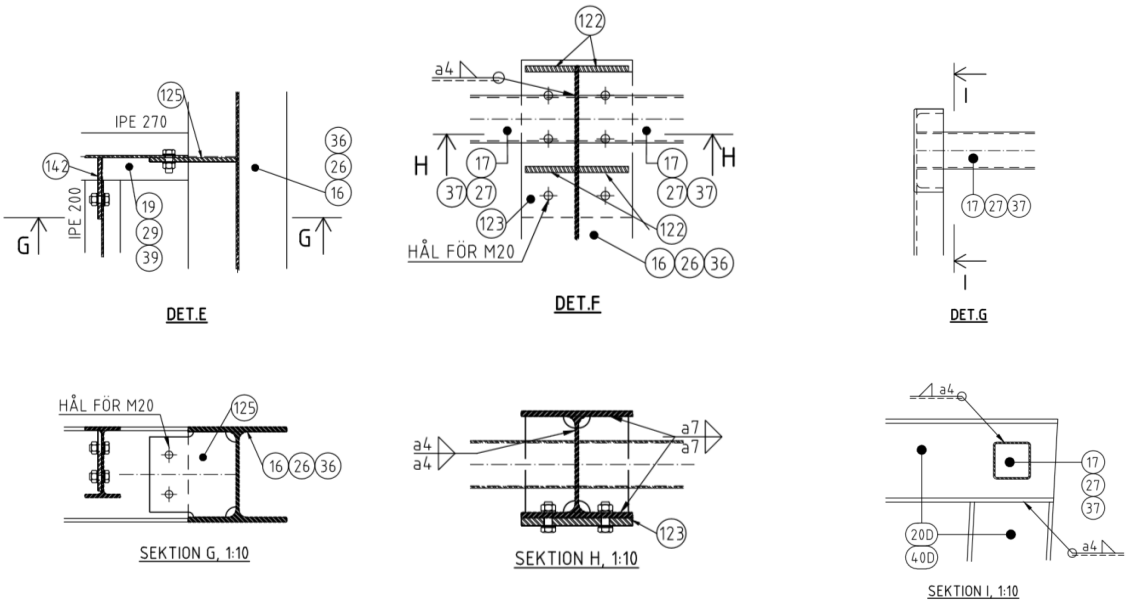

(a) Det. E - partly free, bolted joint.

(b) Det. F - ridig, bolted and welded connection of frame corners.

(c) Det. G - ridgid, welded connection of edge KKRK beams.

Figure 5.14: Various types of joint between elements in the side section of the frame. Placement of joints is shown in Figure 5.12 [7].

Connections in the side sections
Det I: Longitudinal UPE-160 profiles are bolted together with a L-plate attached to the column shown in Figure 5.15a.

Det J: Vertical UPE-160 profiles have welded connections shown in Figure 5.15b.

Det 06: The HEA-280 column base continues through the longitudinal HEA-500 element, (A and H), and are joined together with welded a connections shown in Figure 5.15c .

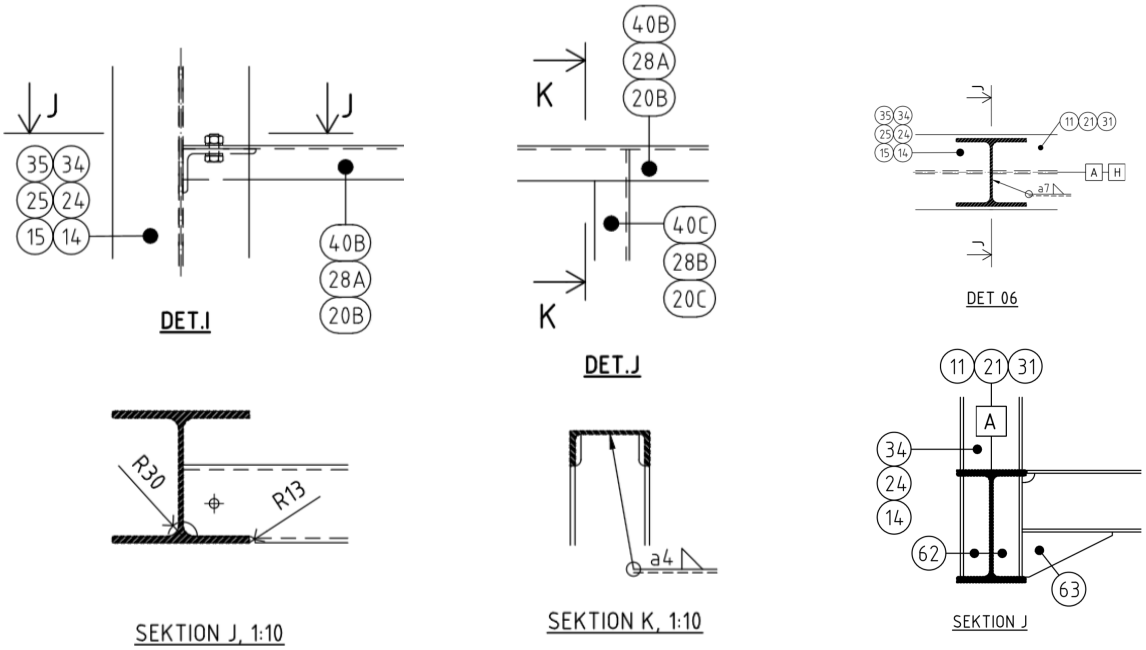

(a) Det. I - partly free, bolted joint of horizontal, intermediate beam elements.

(b) Det. J - ridgid, welded joint of vertical, intermediate beam elements.

(c) Det. 06 - ridgid, welded joint between columns and floor beams.

Figure 5.15: Various types of joint between elements in the side section of the frame. Placement of joints is shown in Figure 5.13 [7].

5.5 Stairwell

The stairwell is built up of vertical VKR- and horizontal UPE beam elements creating a frame structure supporting roof, walls and windows. The floor beams are made up of HEA-120 and HEA-240 beam elements shown in Figure 5.16. The deck has the same cross section as for the main bridge.

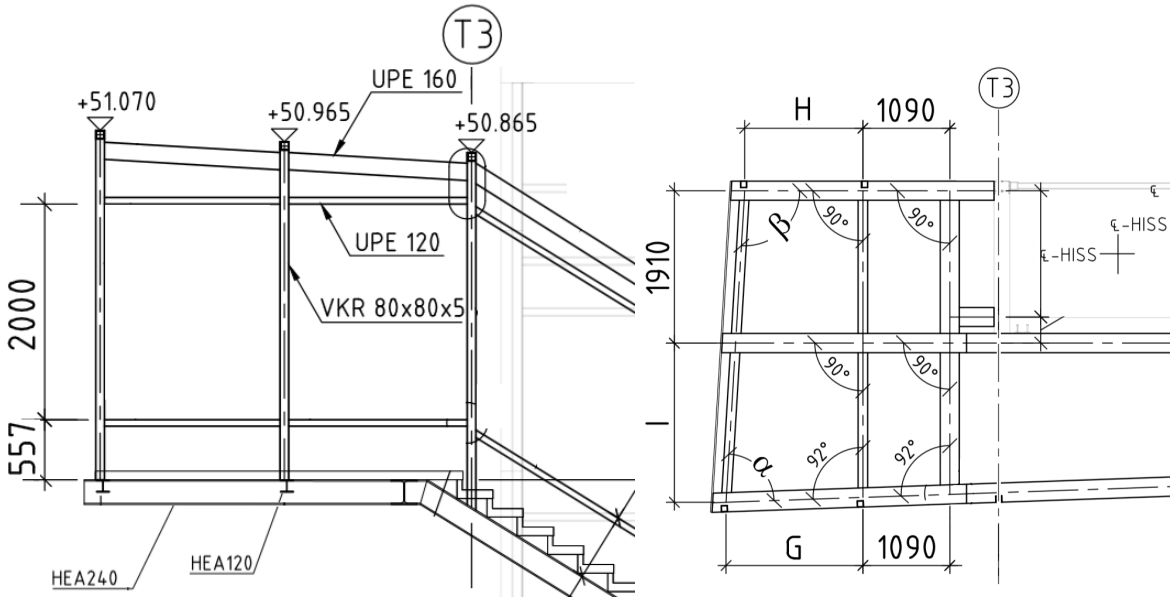

(a) Profile of stairwells connecting to the main bridge. **(b)** Top view of stairwells connecting to the main bridge.

Figure 5.16: Structural members constituting the stairwells connected to the main bridge [7].

Connections - Stairwell
The stairwell is connected to the main deck by a bolted connection. HEA- element of both parts are fitted with a individual steel plate which are bolted together shown in Figure 5.17.

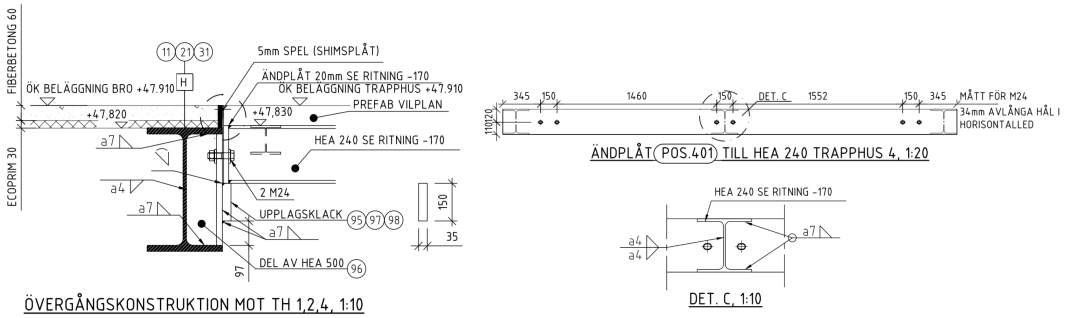

(a) Bolted connection with end plates to floor beams, profile. **(b)** Bolted connection with end plates to floor beams, front view.

Figure 5.17: The joint connecting the stairwells to the edge floor beam [7].

5.6 Facade

The facade consists of corrugated steel and windows constituting a total surface area estimated to 1100 m^2 which are mounted against the frame and intermediate UPE-beam element.

5.6.1 Corrugated steel

The corrugated steel makes up most of the facade surface area at approximate 960 m^2. Manufacture of the corrugated steel used for construction is unknown. Model T130M-75-930 from Ruukki will be used to describe the corrugated steel profile as it is a plausible profile that matches the construction drawings in Figure 5.18 well. Design choices, material data and installation instructions provided from Ruukki is presented for this model.

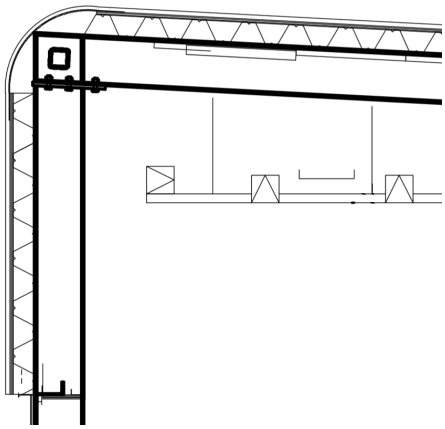

Figure 5.18: Close up of the facade profile and installations [7].

Design options T130M-75-130
Length of the steel sheet can be chosen between 0.8-18.3 m with a effective width of 930 mm. Sheet thickness range from 0.7-1.5 mm with corresponding masses between 9.17-19.36 kg/m^2. A steel sheet with the thickness of 1 mm has a mass of 13.25 kg/m^2

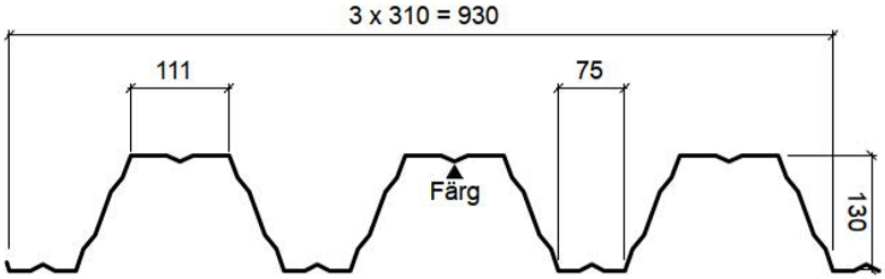

Figure 5.19: Dimensions of the corrugated steel sheets constituting roof and walls. Figure from Ruukki Installation Guide [8].

Instructions for installation
Installation instructions provided by Ruukki requires a minimum overlap of 200 mm for sheet ends, Figure 5.20a and a half wave for side overlapping in 5.20b. Larger overlap can be chosen for both directions depended on desired properties.

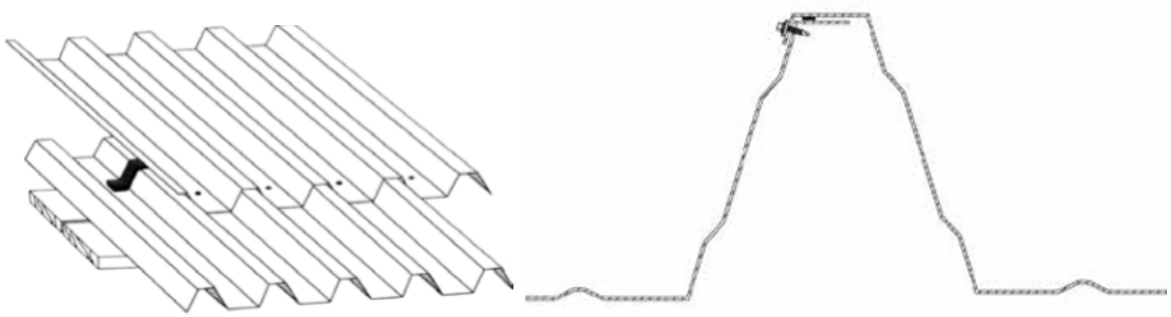

(a) Longitudinal overlap. **(b)** Transversal overlap.

Figure 5.20: Overlap used for installation of the corrugated steel sheets. Figure from Ruukki Installation Guide [8]

5.6.2 Windows

Windows are mounted on both sides, between frame sets, overlooking the tracks in the north and south direction shown in Figure 5.21. The windows have a height of 2 and 1.5 m for the north and south side respectively. Total area are estimated to around 128 m^2. Material of the windows are some kind of polycarbonate with a thickness estimated to 4.5 mm based on inspections. Skylights of dimension 2200x2200 mm are mounted in line with sections across the stairwells, making up a total of 4 skylights.

(a) Windows north side to the left.

Figure 5.21: Windows of the constructed bridge.

5.6.3 Installations

Interior of the superstructure are covered with a wall cladding and a suspended inner-ceiling with lighting, wiring and signs Figure 5.21. Safety railing are installed along sides of the ramp and at open cross section, facing east, of the main bridge.

5.7 Supports

The deck rest on eleven point-supports placed on five separate abutments, marked 1-4 and R1 in Figure 5.22. Top row of supports, marked in blue, allows for movement in the longitudinal- and transverse direction. The bottom left support, marked in red, is pinned and thereby the reference point with zero displacement. Supports marked in cyan allows movement in the longitudinal direction.

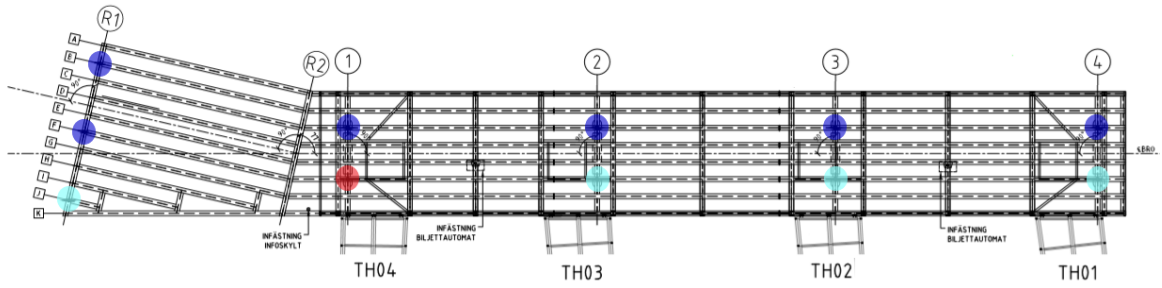

Figure 5.22: Supports placed along center lines 1-4 and R1 [7].

5.8 Material properties

This section presents an inventory of material, quantity and quality of main elements in the constructed bridge. All steel used for construction are prescribed to be structural steel of execution class XC3 or higher, according to the construction drawings. An overview of total mass and quantity for walkways, facade and beam element is presented in Table 5.1 further divided for individual element in following sub-chapters. Total mass of the bridges superstructure excluding installations and connecting stairwells is approximate 246 ton, Figure 5.23 and Table 5.1.

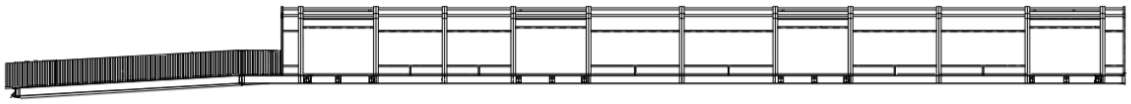

Figure 5.23: Sideview of the complete bridge [7].

Table 5.1: Overview of quantity and mass distribution of elements in the bridge.

Element	Quantity	Total Mass [ton]
Beam	1206 m	120.1
Deck	504 m^2	112.9
Facade	1088 m^2	13.4

Beam members
All beam members makes up a total length 1206 m with a mass of 120.1 ton summed up from Table 5.2.

Table 5.2: Beam profiles and corresponding mass, quantity and steel grade.

For	Quantity [m]	Mass [kg/m]	Total Mass [ton]	Steel grade
HEA280	245	76.4	18.7	S355J2G3
HEA500	609	155.1	94.4	S355J2G3
IPE200	8	22.4	0.1	S355J2G3
IPE270	18	36.1	0.7	S355J2G3
KKRK	111	17.6	1.9	S355J2G3
UPE160	184	17.0	3.1	S355M
UPE270	31	35.2	1.1	S355M

Deck
Weight of the combined cross section of the deck is 224 kg/m^2 resulting in a total mass of 112.9 ton for the combined 504 m^2 surface area, summed up from Table 5.3.

Table 5.3: Material, quantity and mass of the deck.

For	Type/grade	Thickness [mm]	Density [kg/m^3]	Mass [kg/m^2]	Total Mass [ton]
Concrete	C35/45, XD1, fiber reinforced	60	2410	144.60	112.5
Isolation	Polystyrene (XPS)	30	28	0.84	0.4
Steel	S355	10	7850	78.50	39.6

Facade
Total weight of the facade is estimated to 13.4 ton with a surface area of 1088 m^2 summed up from Table 5.4. Weight of the corrugated steel is increased slightly due to overlap of the steel sheets at assembly.

Table 5.4: Properties, quantity and mass of the facade.

For	Thickness [mm]	Density [kg/m^3]	Weight [kg/m^2]	Area [m^2]	Total Mass [ton]
Corrugated steel	1	-	13.25	960	12.7
Windows	4.5	1200	5.4	128	0.7

6 Measurements

This chapter presents setup of equipment and results obtained from acceleration measurements for one of the sections of Skyttelbron.

6.1 Method

The primary goal of the acceleration measurements was to obtain natural frequencies and mode shapes for the constructed bridge. Accelerometers were placed on the deck of the longest span of the bridge, which is span 3. Accelerations were then recorded in the time domain for 4 seconds while exciting the bridge with an impact hammer. Each excitation point was excited 3 times with sufficient coherence to obtain accurate data.

6.1.1 Setup and Equipment

Equipment used for measurements are from Brüel Kjær. Piezoelectric CCLD Accelerometer of type 4507 used to measure accelerations are shown in Figure 6.2a placed in point S1-S3 according to Figure 6.1. Heavy-duty Impact Hammer of type 8210 used to excite the bridge in points E1-E7 is shown in Figure 6.2b. Accelerometers and impact hammer were connected to a signal conditioner, LAN-XI Data Acquisition type 3050-A-060 shown in Figure 6.2c.

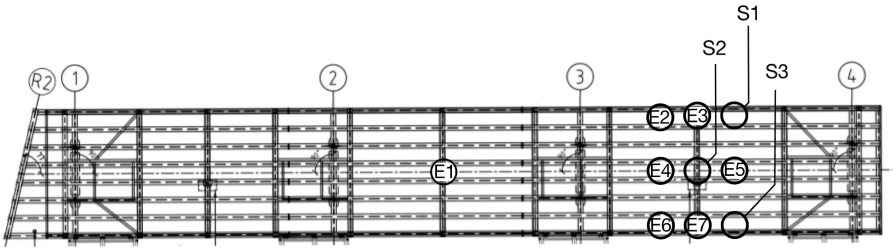

Figure 6.1: Location of accelerometers and excitation points on the deck of main span 3 [7].

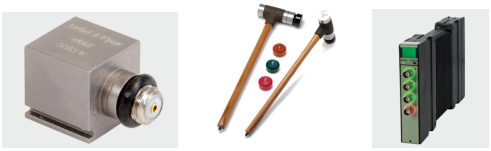

(a) Accelerometer. **(b)** Impact Hammer. **(c)** Front-end.

Figure 6.2: Equipment used for measurements. Pictures from Brüel Kjær [9]

6.2 Results

Post processing of measurements resulted in natural frequencies, mode shapes and the FRF of each measurement.

6.2.1 Natural frequencies

Modes of interest is modes with natural frequency close to the walking range, preferable with a low complexity. They were identified primary as mode 1 and 2 but also mode 5 all shown in Table 6.1.

Table 6.1: Result from measurements, natural frequencies of Skyttelbron

Mode	Damped Frequency [Hz]	Damping [%]	Complexity
1	5.55921	4.17049	0.0763
2	7.42909	4.91667	0.00904
3	11.07318	4.51382	0.93851
4	14.04572	4.07024	0.3113
5	14.32078	4.61916	0.03725
6	17.23853	4.81945	0.23498

6.2.2 Mode shapes

Mode shapes identified as the primary to modes of interest are shown in Figure 6.3.

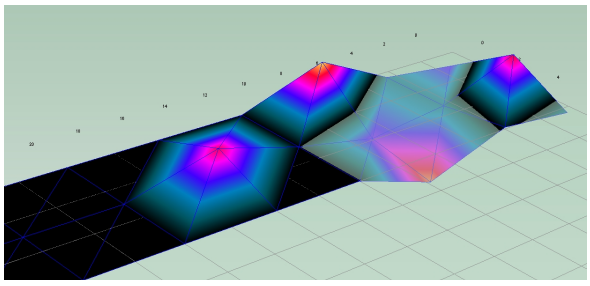

(a) Mode 1.

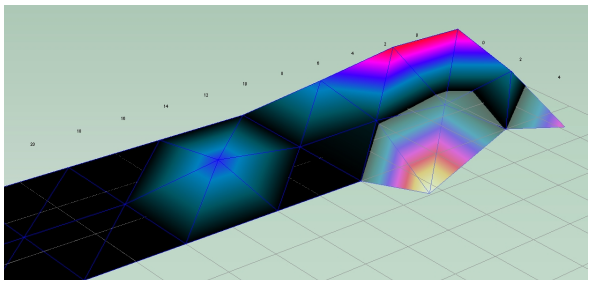

(b) Mode 2.

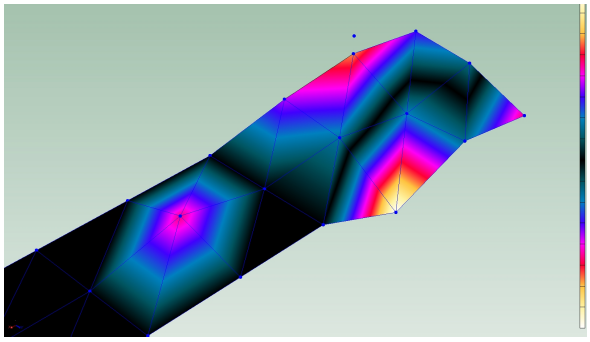

(c) Mode 5.

Figure 6.3: Mode shapes for modes of interest.

6.2.3 Frequency Response Function

Accelerations in the time domain have been converted to the frequency domain by the FFT method and then normalized by the magnitude of the load. The FRF of respective excitation point and accelerometer, S1-S3, is plotted as the mean value of all FRFs for each accelerometer in Figure 6.4.

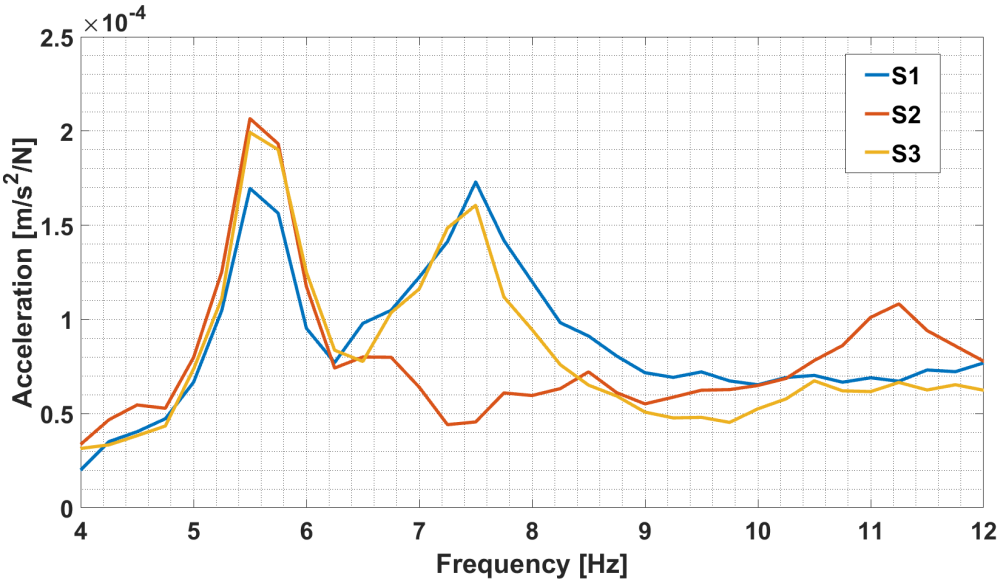

Figure 6.4: Mean value of all FRFs for each accelerometer, S1-S3.

6.3 Discussion

While measuring accelerations there were some disturbances from people crossing the bridge including the 4 people conducting the measurements contributing with some small mass that may reduce the natural frequencies of the bridge. There were also some issues recording measurements from one of the excitation points. This is believed to cause the odd shape of point E7 in the mode shapes. Despite this, there is high confidence in the measured data, especially for the first two modes showing a low complexity.

7 FE-model

This chapter describes the Finite Element models designed using the FE-software Abaqus.

7.1 Model 1 - Reference model

The complete FE-model is shown in Figure 7.1 and broken down to smaller parts in subsections describing properties, geometry, constraints and nonstructural mass in greater detail. Constraints are marked with a yellow circle in figures and is modeled in two versions representing a moment stiff- or free joint. Both versions tie together translations while the rigid joint also ties together rotational DOFs. Nonstructural mass is illustrated by a green mark and is just shown partly not to cover the constraints.

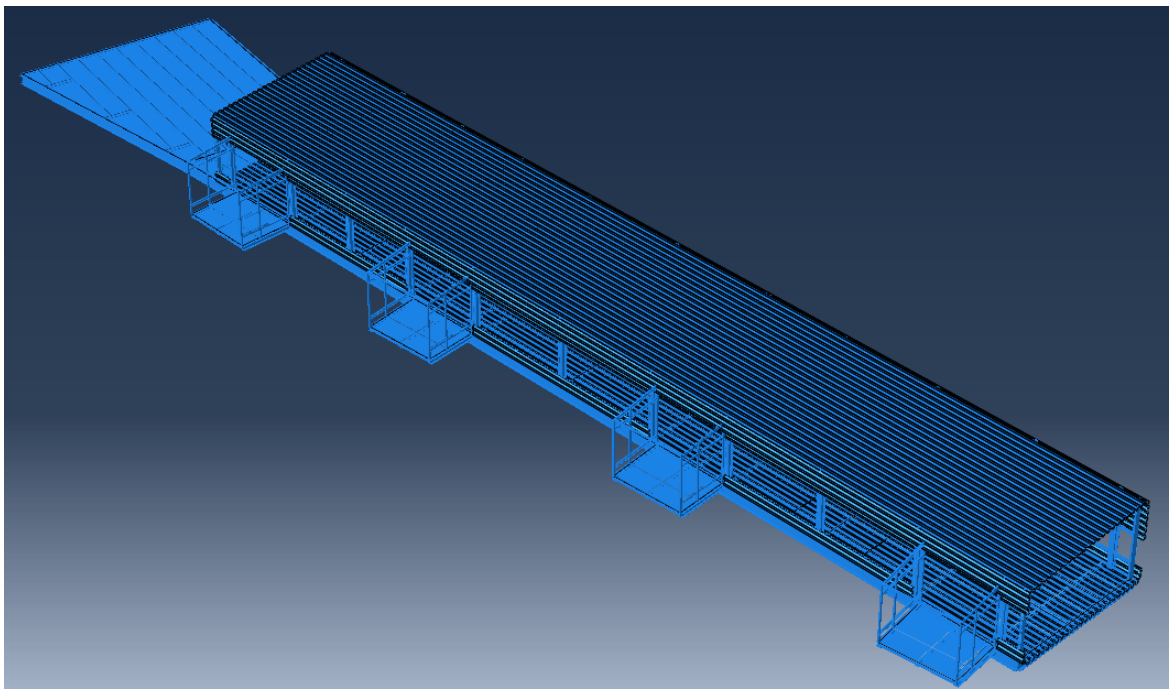

Figure 7.1: Overview of the complete FE-model.

7.1.1 Parts

Floor beams
Floor beams of the bridge, built as one part with beam elements, are shown in Figure 7.2. Floor beams with HEA500 and HEA280 profiles makes up a mass of 93 and 5 tons. Close up of span 1 displaying the beam profiles in Figure 7.3.

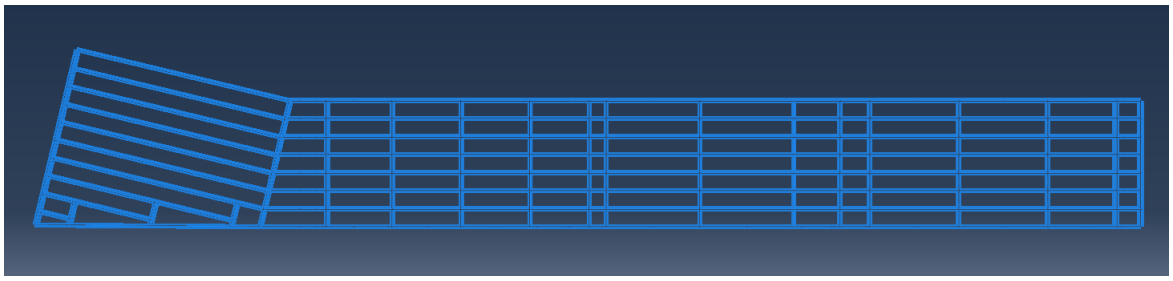

Figure 7.2: Overview of the floor beams consisting of HEA500 and HEA280 profiles.

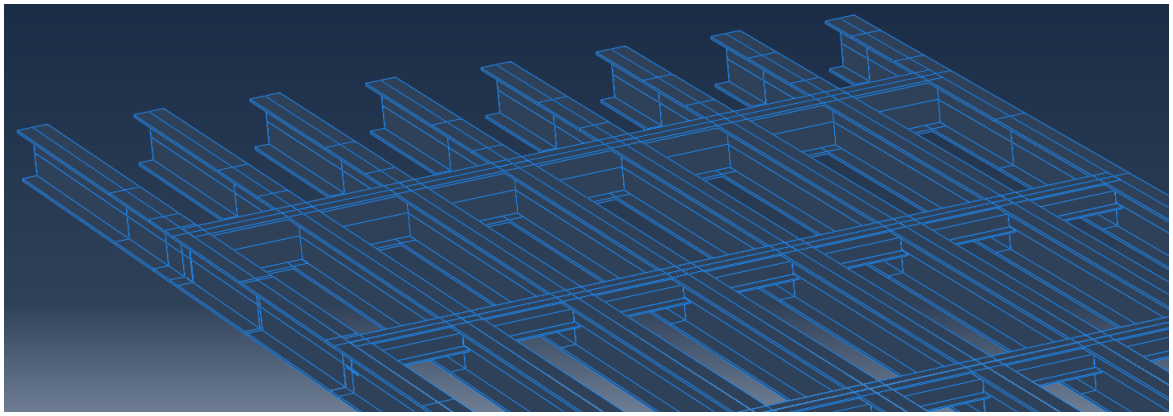

Figure 7.3: Close up of span 1, highlighting the different dimensions of the HEA500 and HEA280 profiles.

Ramp
Connection between the ramp and span 1 consists of rigid node-to-node tie constraints. Span 1 constitutes the leading part, shown in Figure 7.4.

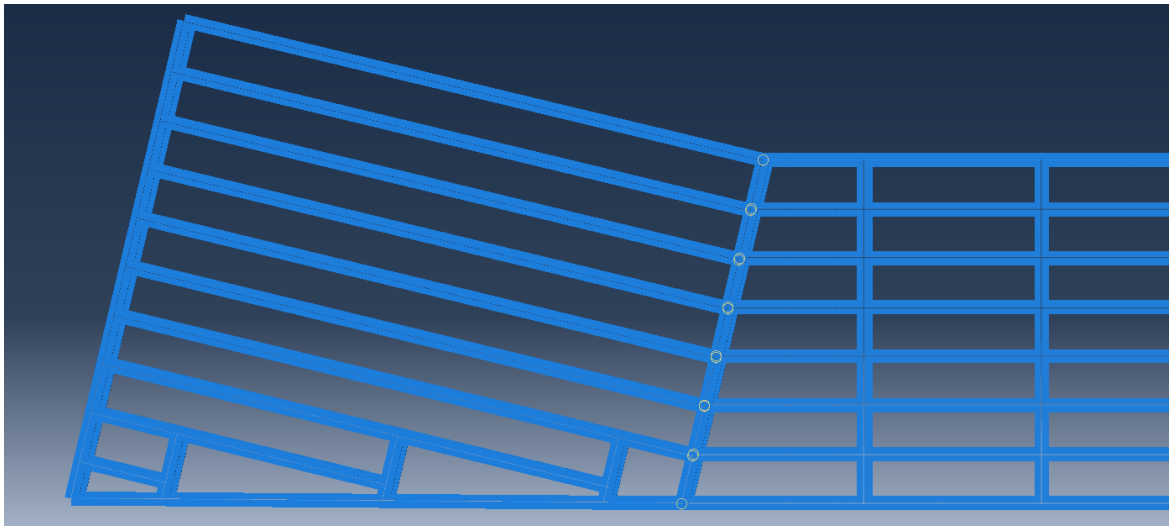

Figure 7.4: shows an overview of the Ramp together with the rigid node-to-node tie constraints, marked with yellow circles, against Span 1.

Deck
The deck consisting of three separate layers, are modeled as one shell element, Figure 7.5b, connected to the floor beams through a rigid, surface-to-surface tie constraints, Figure 7.5a, where the floor beams constitutes the leading part. The deck makes up at total surface area of 504 m^2 with a mass of 113 tons.

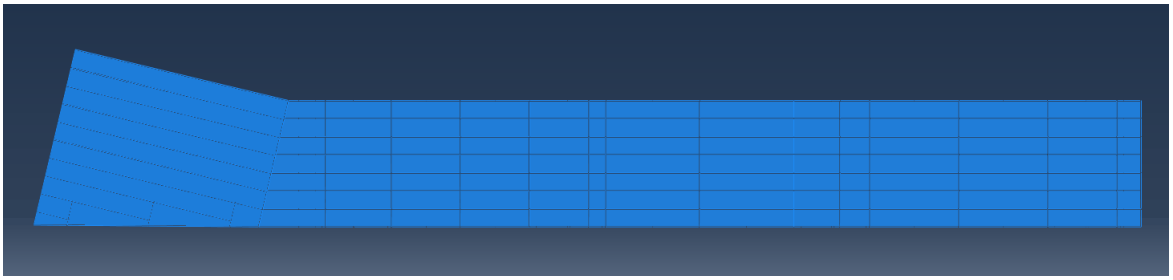

(a) Top side of the deck.

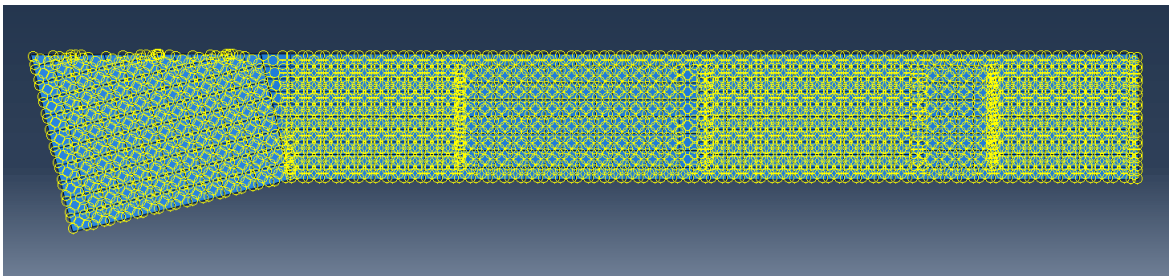

(b) Bottom side of the deck showing constraints against of the surface marked in yellow.

Figure 7.5: Overview of the deck connected to the floor beams through a rigid surface-to-surface tie constraint.

Superstructure
HEA-280 beam frame and intermediate, stabilizing elements carrying up the facade, windows and installations are shown in Figure 7.6. All beam profiles make up a total mass of 22 ton.

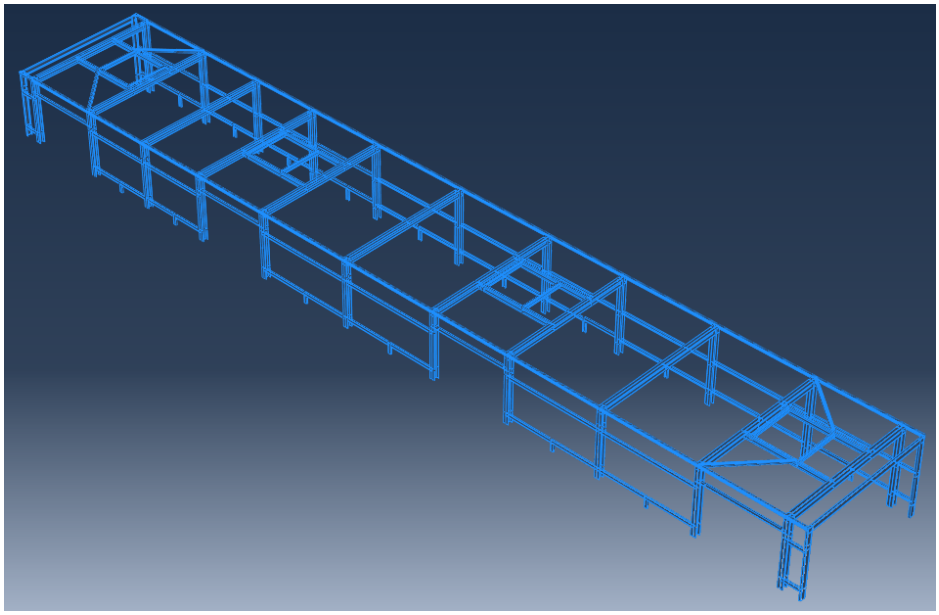

Figure 7.6: Overview of the frame and intermediate, stabilizing beams consisting of HEA280, IPE and UPE profiles.

HEA280 beam frame
HEA-280 beam elements constituting the dram, shown in Figure 7.7. Members are connected together in top corners by a rigid, node-to-node tie constraints representing the bolted connection described in Chapter 5.4. Beam elements of the frame makes up a total mass of 14 tons and carries a non-structural mass of 44 ton to represent the extra weight of installations, bolts, welds etc.

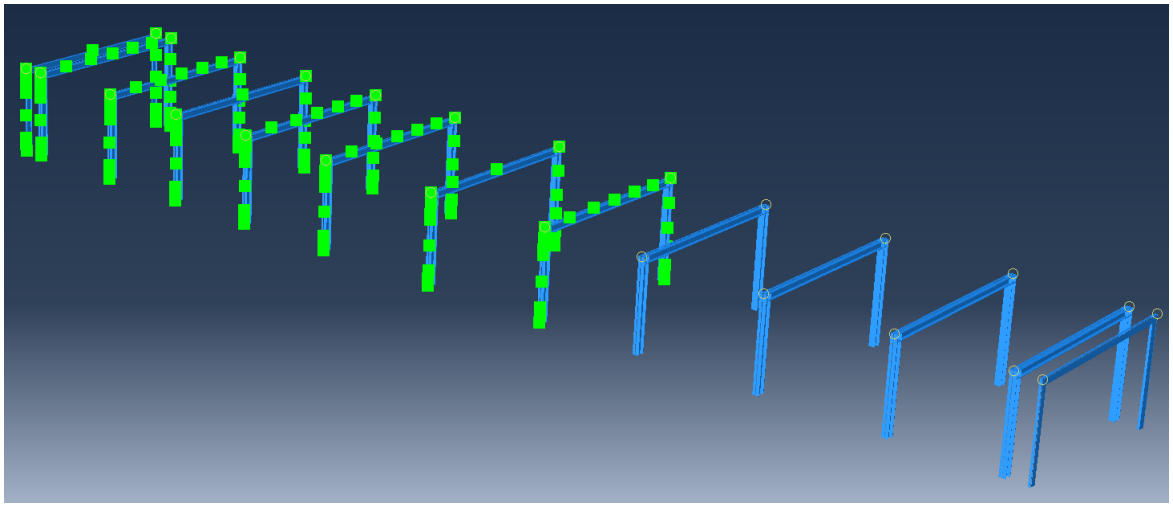

Figure 7.7: Close up of the frame with the rigid, node-to-node constraint marked in yellow.

Intermediate side beams
Intermediate side beams consist of UPE-160 beam elements connected to the columns by a free, node-to-node tie constraints. This allows for rotation in the joint, representing a semi-free bolted connection described in Chapter 5.4. The UPE-160 beams make up a total mass of 4.5 ton and carries the non-structural mass of the windows, 0.8 ton.

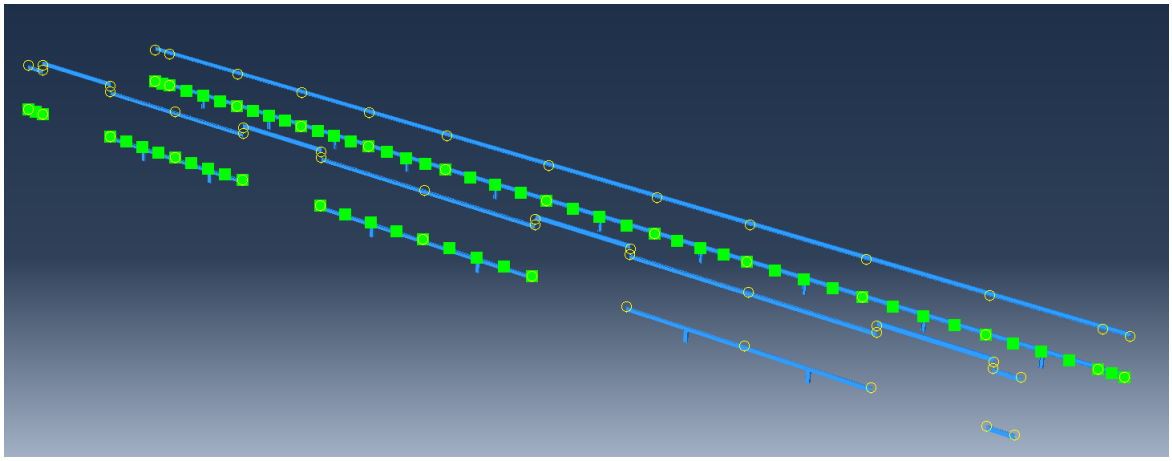

Figure 7.8: Intermediate side beams connected to the frame with a free node-to-node constraint marked in yellow.

Edge beams
Top edge beams, consisting of 120x120 mm KKRK beams are shown in Figure 7.9. They are connected to the frame by a rigid, node-to-node tie constraints to represent a welded joint described in Chapter 5.4. Total mass of edge beams is 1.8 ton.

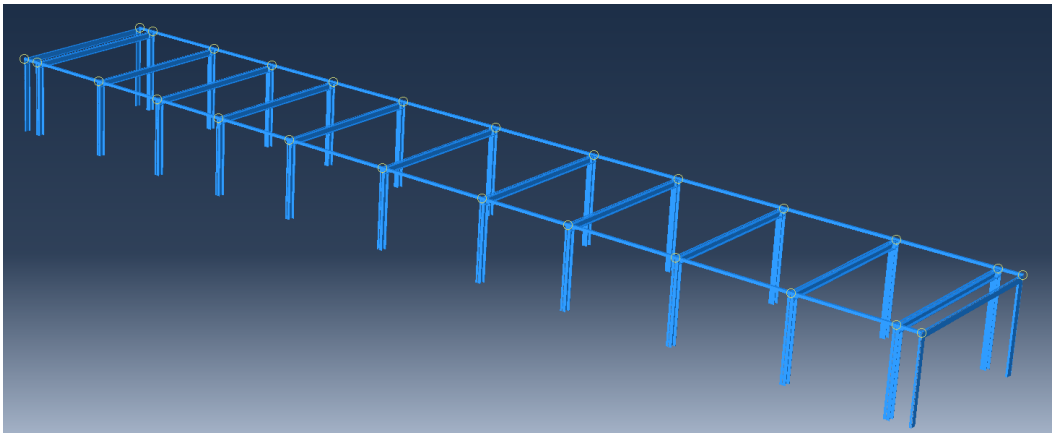

Figure 7.9: Edge beams with a KKRK-profile connected to top corners of the frame by a rigid, node-to-node connection marked in yellow.

Intermediate top beams
Intermediate top beams are consisting of IPE- and KKRK beam elements connected to the frame by a free, node-to-node tie constraints. This to represent a semi-free, bolted joint described in Chapter 5.4. IPE- and KKRK beam elements makes up a total mass of 2.0 ton and carries the non-structural mass of the skylights 0.14 ton.

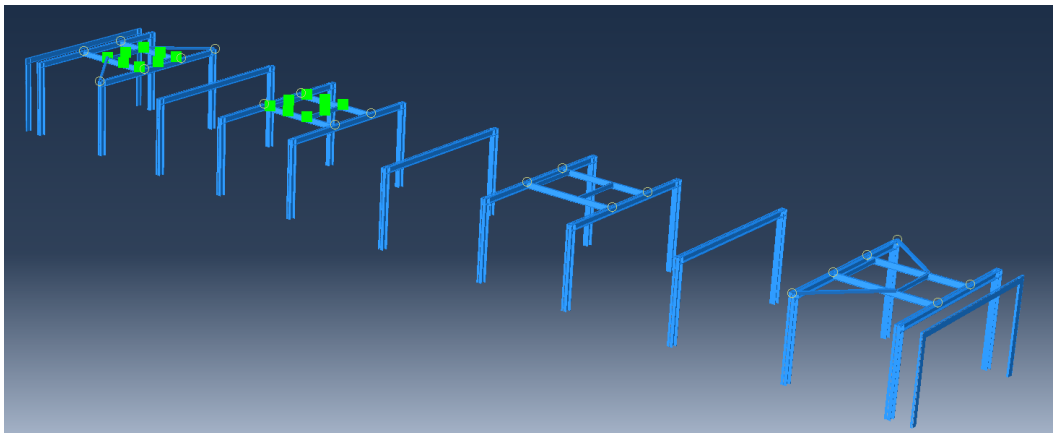

Figure 7.10: Intermediate top beams with IPE- and KKRK-profiles connected to the frame by a free, node-to-node connection marked in yellow.

Stairwells
Stairwells are modeled to improve boundary conditions otherwise representing the substructure connecting bridge to the tracks. They are modeled as one part with internal members consisting of HEA-120, HEA-240, UPE- and VKR beam elements. These constitutes floor beams, frame and deck, shown in Figure 7.11, making up a total weight of 15.2 ton. The stairwell is connected to the main floor beams and intermediate UPE side-beams by a rigid- and free, node-to-node tie connection.

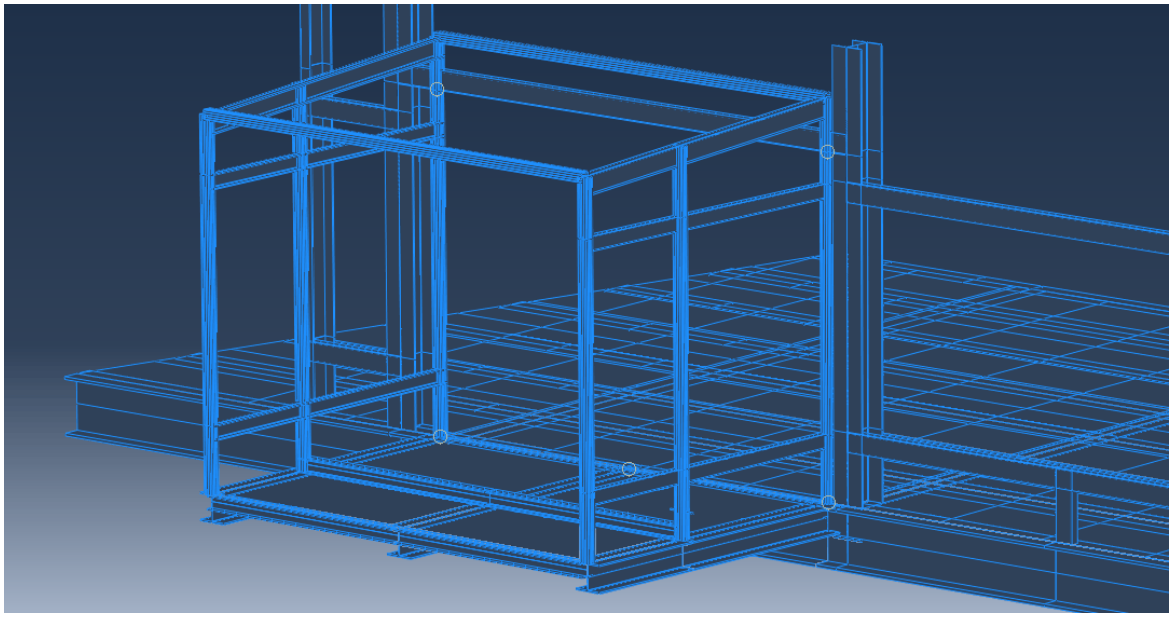

Figure 7.11: Stairwell connected to main bridge with rigid and free tie constraints in the bottom and top respectively marked in yellow.

Facade

The facade is simplified for the FE-model solely represented by corrugated steel, modeled after Ruukkis product data of model T130M-75-130 shown in Figure 7.12c. It is modeled with 1 mm, extruded shell elements and profile shown in Figure 7.12a. The shell elements are connected to the frame, intermediate- and floor beams by a rigid, surface-to-surface constraint shown in Figure 7.12b. The corrugated steel makes up a total shell area of 1459 m^2 with a weight of 13 tons.

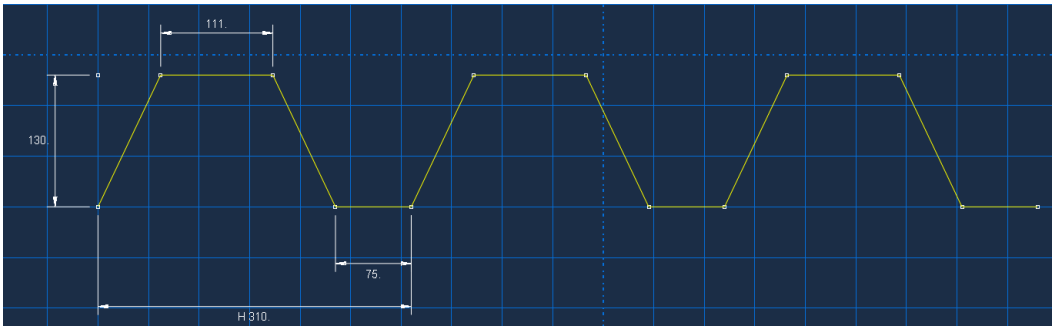

(a) Dimensions of the extruded shell profile according to Ruukki model T130M-75-130.

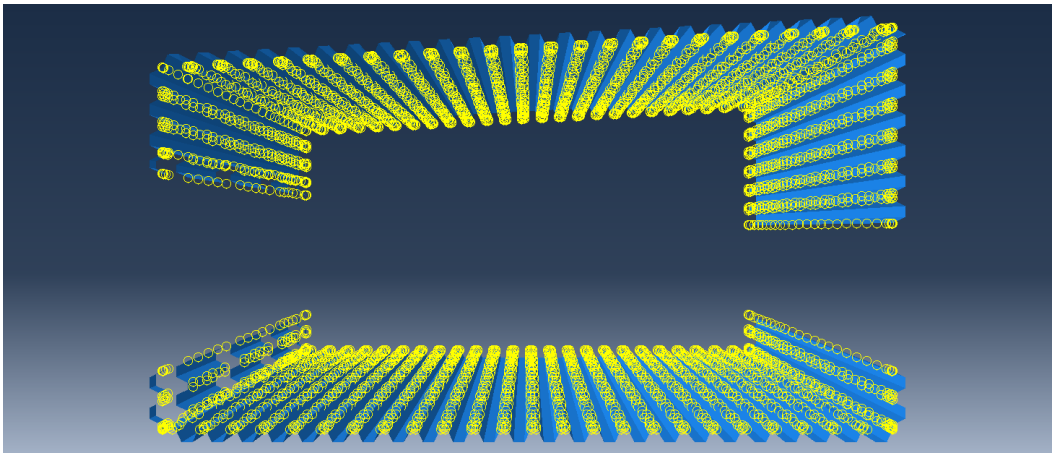

(b) Surface-to-surface constraints of the corrugated steel marked in yellow.

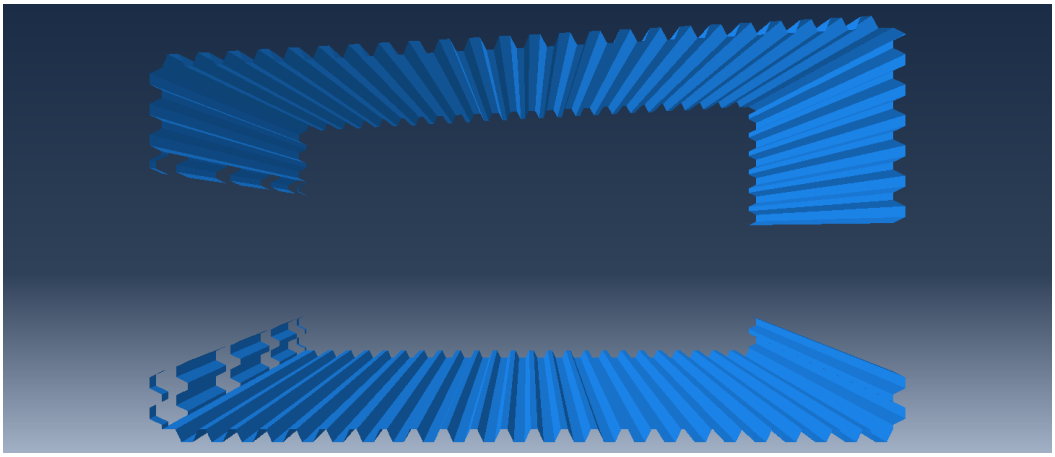

(c) Corrugated steel.

Figure 7.12: Profile and constraint of shell elements representing the corrugated steel facade.

7.1.2 Boundary conditions

Three types of boundary conditions, pinned, vertically restricted, vertically- and transversally restricted, are used to represent the support conditions described in chapter 4.8, shown in Figure 7.13a. In addition boundary conditions are also placed by the stairwell in connection to the concrete elevator shaft, represented by the same three boundary conditions shown in Figure 7.13b and 7.13c.

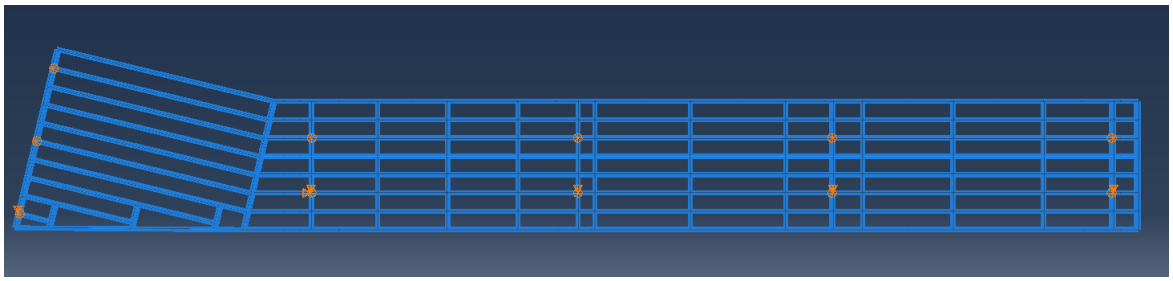

(a) Boundary conditions representing the supports.

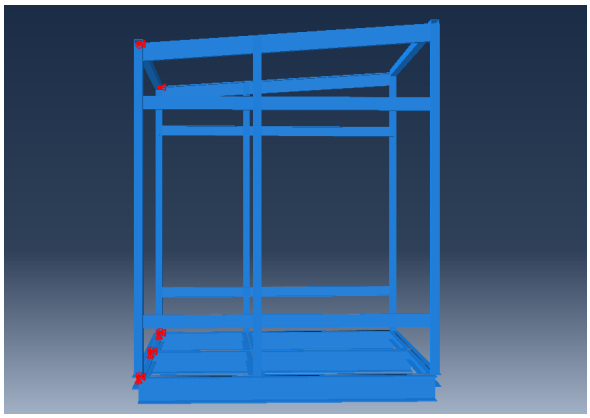

(b) Boundary condition applied to secondary structure, Stairwells.

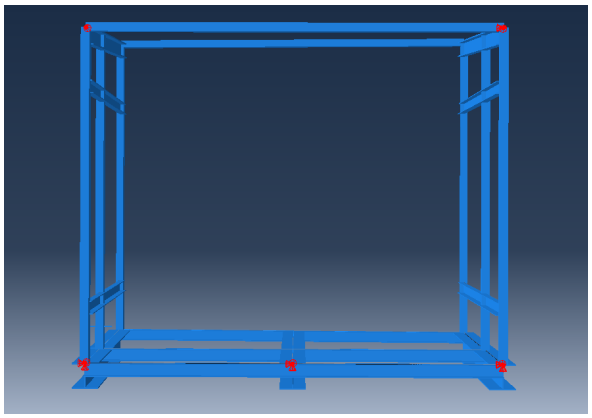

(c) Boundary condition applied to secondary structure, Stairwells.

Figure 7.13: All boundary condition, representing support conditions together with connections to secondary structure excluded in the model.

7.1.3 Summary of FE-model

Mass
Total mass of the numeric model amounts to 322 tons distributed on model members as shown in Table 7.1. Mass of beam members, deck and corrugated steel is generated in Abaqus based on material density.

Table 7.1: Mass distribution of model members.

Part	Mass [10^3 kg]	of total mass
Floor beams	98	30%
Deck	113	35%
Frame	14	4%
Intermediate beams	8.3	3%
Facade	13	4%
Stairwell	15.2	5%
Sum:	261.2	81%

Non structural mass
Parts of the bridge not affecting to the stiffness is modeled as a non-structural mass to account for the contribution to the dynamic response. Masses from bolts, welds, installations etc. is modeled as a line- or surface load applied according to Figure 7.14 with total quantities from Table 7.2.

Table 7.2: Total non-structural mass applied in the model.

	Load type	Mass [10^3 kg]	of total mass
Installations	Line load	44	14%
Deck	Uniform	15.5	5%
Windows	Line load	1	0%
Sum:		69.5	19%

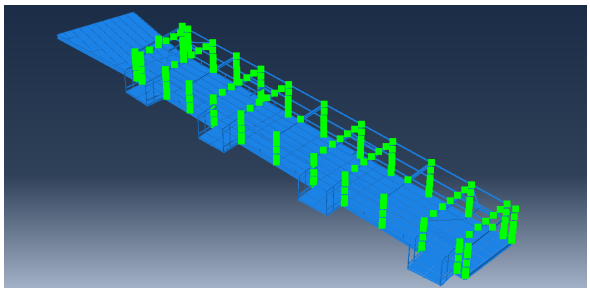

(a) Non-structural mass from installations, 227 kg/m.

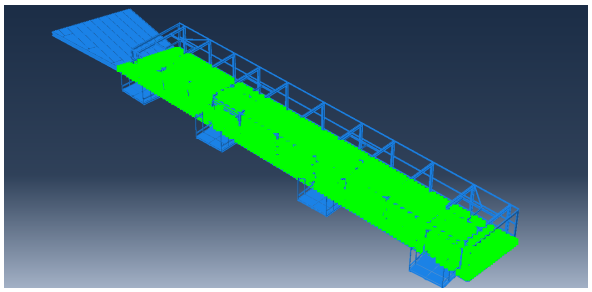

(b) Non-structural mass from installations, 40 kg/m^2.

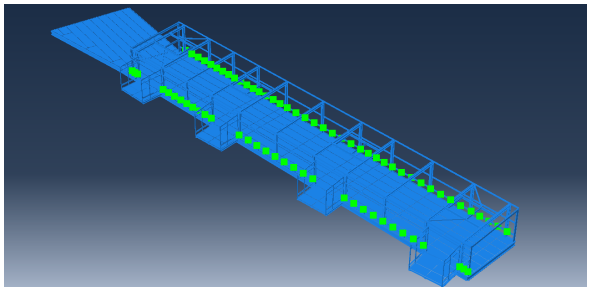

(c) Non-structural mass from windows, 11 kg/m.

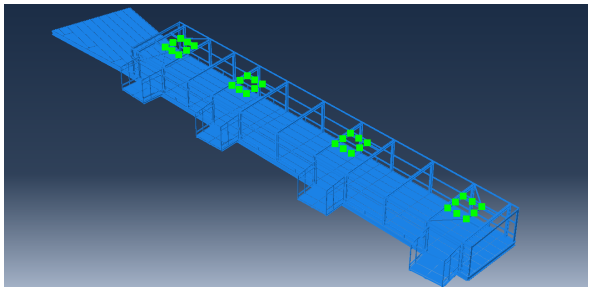

(d) Non-structural mass from windows, 11 kg/m.

Figure 7.14: Distribution of non-structural mass.

Part properties
All parts have been modeled as a steel material with the E-modulus of 210 GPa and Poisson's ratio of 0.3. Concrete in the deck is assumed not to contribute to the stiffness due to lack of interaction between the concrete and steel plate. Density of the steel plate is adjusted to account for the extra mass. The corrugated steel have a density to account for the shape in order to achieve the the weigh of 13.25 kg/m^2 as described in Chapter 5.6. Summary of beam and shell element shown in Table 7.3 and 7.4.

Table 7.3: Beam elements of the FE-model.

Element	Profile	Material
HEA500	I-	Steel
HEA280	I-	Steel
HEA240	I-	Steel
HEA120	I-	Steel
IPE200	I-	Steel
IPE270	I-	Steel
UPE120	U-	Steel
UPE160	U-	Steel
UPE270	U-	Steel
KKRK	Square	Steel
VKR	Square	Steel

Table 7.4: Shell elements of the FE-model.

Section	Element	Thickness [mm]	Material	Density [kg/m^3]
Deck	Shell	10.0	Steel	2240
Corrugates steel	Shell	1.0	Steel	8676

7.2 Model 2 - HEA400

In **Model 2**, primary load bearing HEA500 beam elements are exchanged to a HEA400 profile. The exchange results in a reduction of mass and stiffness. Final Weight of **Model 2** amounts to 303 tons a reduction of 6 %.

7.3 Model 3 - Reduced model

In **Model 3**, the corrugated steel representing the facade is removed completely and the mass is compensated to keep the total mass unchanged. Corrugated steel removed is shown in Figure 7.15.

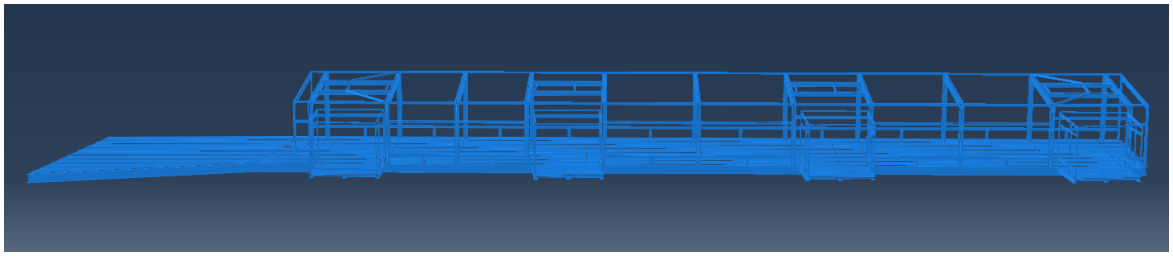

Figure 7.15: Model 3 where the corrugated steel is removed.

7.4 Parametric study

Parameters in the reference model, **Model 1**, is changed individually to compare their effect on the dynamic response of the FE-model. Reference- and adjusted value for alternative 1-3 is shown in Table 7.5.

Table 7.5: Overview of parameters alternated while conducting the parametric study.

Parameter	**Reference**	**Alt. 1**	**Alt. 2**	**Alt. 3**
Corrugated steel	1 mm	2 mm	5 mm	Removed (Model 3)
Deck	10 mm	15 mm	25 mm	-
Intermediate beams	Free rotation	Locked rotation	Inc. E-module	Removed
Mass quantity	45 Ton	68 Ton	90 Ton	Removed
Mass distrubution	Line mass	PM-top	PM-bot	Uni.Mass-deck

Stiffness
Higher stiffness of the corrugated steel and deck were achieved by increasing shell thickness of respective part in alternative 1-3. Stiffness of intermediate beams were increased by adding more restraints, locking the rotational DOFs in tie connection to the frame and by a increased E-modulus.

Mass properties
The effect of mass quantity were tested by altering the line load in Figure 7.16a, the non-structural mass representing unknown mass of installations etc. according to Table 7.6. Effect of mass distribution were investigated by moving the line load in Figure 7.16a, while keeping the total mass constant, to point loads place according to Figure 7.16b and 7.16c as well as a uniform distributed load over the whole deck.

Table 7.6: Total- and line load mass changes, investigating the effect of mass quantity on the FE-model.

	Reference	**Alt.1**	**Alt.2**	**Alt.3**
Line load [kg/m^2]	227	0	340	454
Total Mass [ton]	322	277	344	366

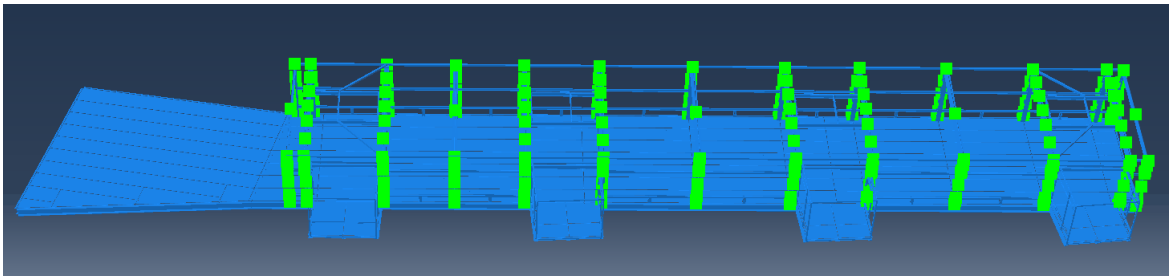

(a) Original placement of non-structural mass in the reference model, Model 1.

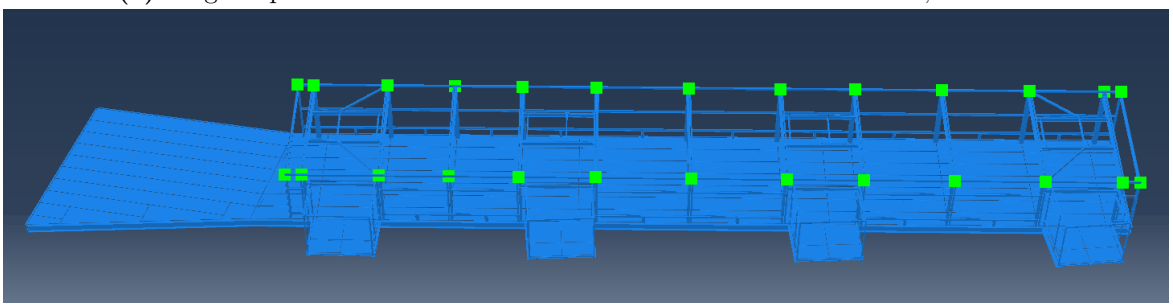

(b) Alternative placement of mass as point mass in column tops of the frame, 1725 kg per point.

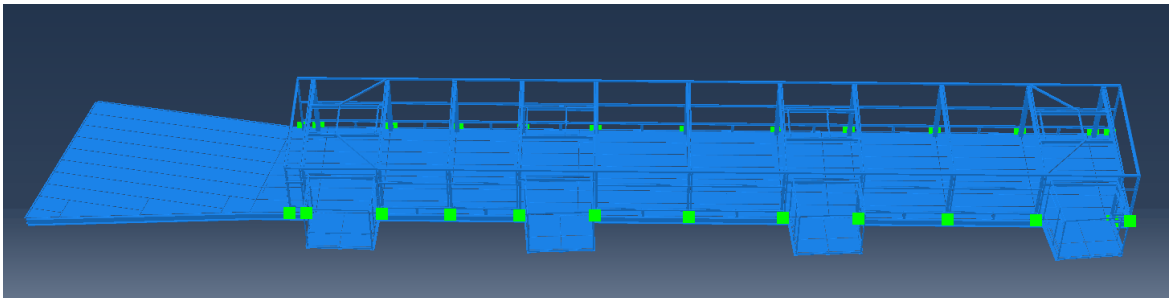

(c) Alternative placement of mass as point mass in column bottoms by the floor beams, 1725 kg per point.

Figure 7.16: Alternative distribution of non-structural mass.

8 Numerical studies and results

In this chapter the results from the parametric study and dynamic analyses of respective model according to Sétra are presented.

8.1 Dynamic analysis

The dynamic analysis is primarily focusing on natural frequencies below 10 Hz causing resonance in the deck. Natural frequencies and mode shapes are obtained through an eigenvalue analysis described in Chapter 8.1 with theory from 2.1. Frequencies of interest are singled out by evaluating where peak accelerations occur in the frequency domain, using the FRF where natural frequencies triggering resonance is easy to distinguish.

FRFs were obtained through frequency sweeps using SSD modal analysis with modal damping corresponding to measured damping values. The acceleration response in S1-S3 Figure 8.1, are plotted in the frequency domain as the mean value of FRFs from loading in points E1-E7.

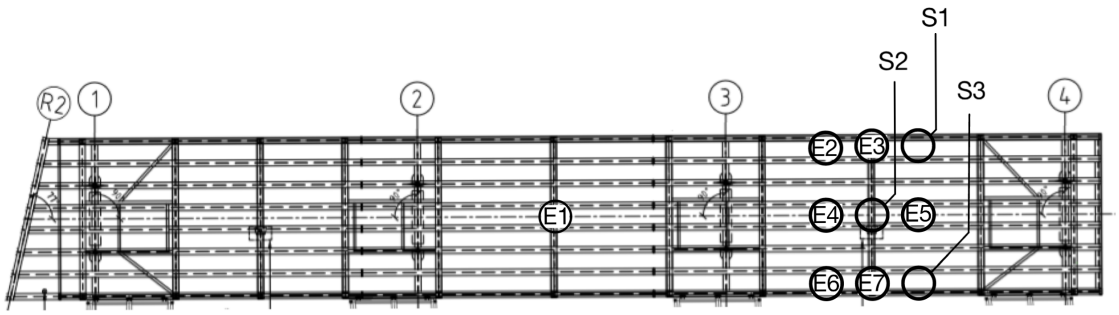

Figure 8.1: Displays excitation- and measurement points for the FRF's [7].

8.1.1 Model 1: Reference model

Natural frequencies and mode shapes
First eight natural frequencies of **Model 1**, obtained through a eigenvalue analysis, is presented in Table 8.1 together with frequencies of mode 21 and 29, later shown to be frequencies of interest. Mode shapes corresponding to mode 1-6 is displayed in Figure 8.2.

Table 8.1: The first natural frequencies of Model 1.

Mode	**Frequency** [Hz]
1	4.06
2	4.97
3	5.02
4	5.16
5	5.31
6	5.57
7	5.95
8	6.09
21	7.59
39	9.15

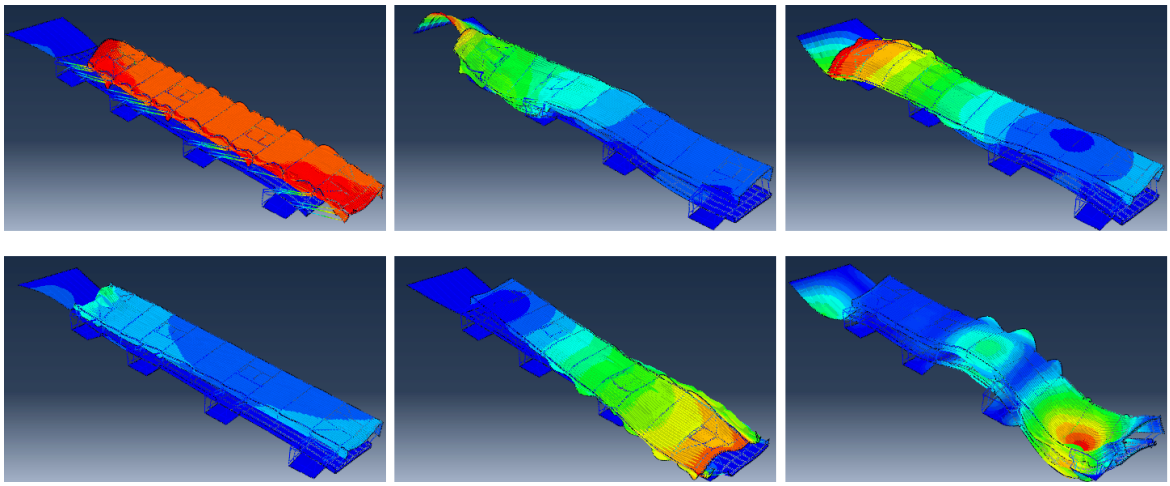

Figure 8.2: Mode shape corresponding to natural frequencies 1-6 in table 8.1

Frequency Sweep
Natural frequencies of interest, causing resonance in the deck are identified from peak accelerations in the FRF in Figure 8.3, from a vertical load exciting modes below 40 Hz. Natural frequencies is found at 5.57, 7.59 and 9.15 Hz corresponding to mode 6, 21 and 39 in Table 8.1.

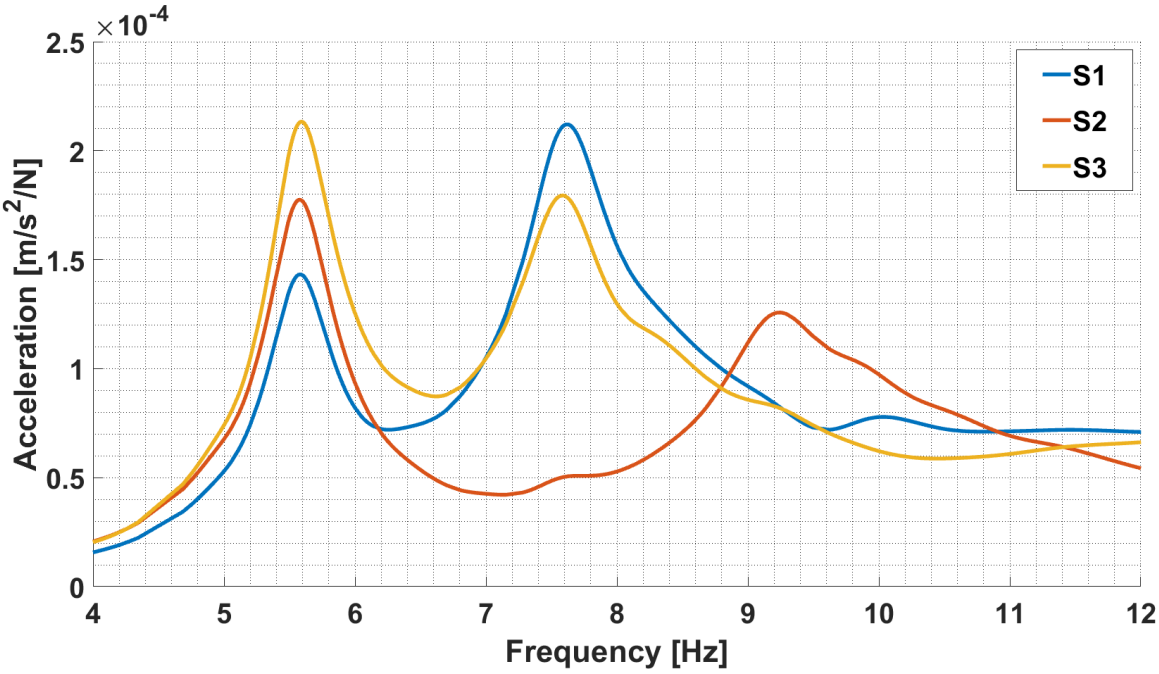

Figure 8.3: FRF of point S1-S3 in **Model 1** as mean value from exciting point E1-E10 with a normalized point load.

Resonance mode shapes
Mode shape corresponding to natural frequencies triggering resonance in the deck mode 6, 21 and 39, is shown in Figure 8.4.

Mode 6: is primary a bending mode but also contains a slight twisting motion.

Mode 21: is a pure twisting mode.

Mode 39: is a combination of bending and twisting where span 3 is affected purely by bending and span 2 contains a twisting motion.

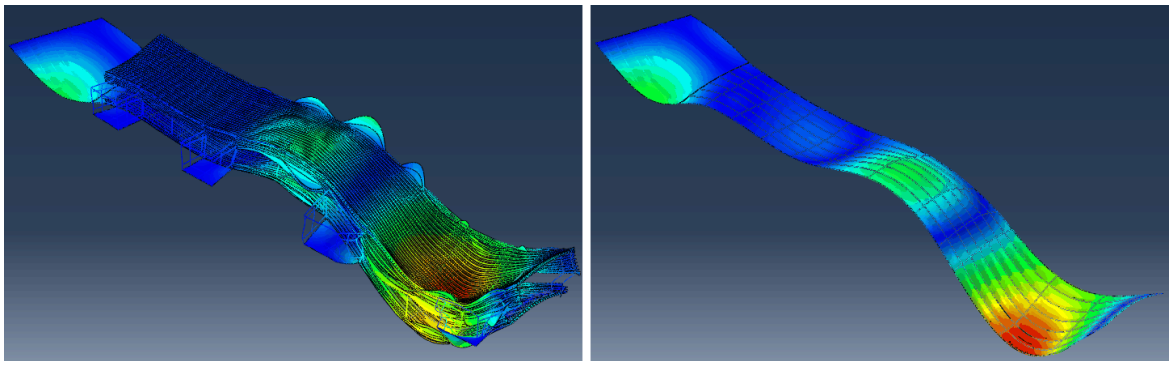

(a) Mode 6 found at 5.57 Hz, primary a bending mode.

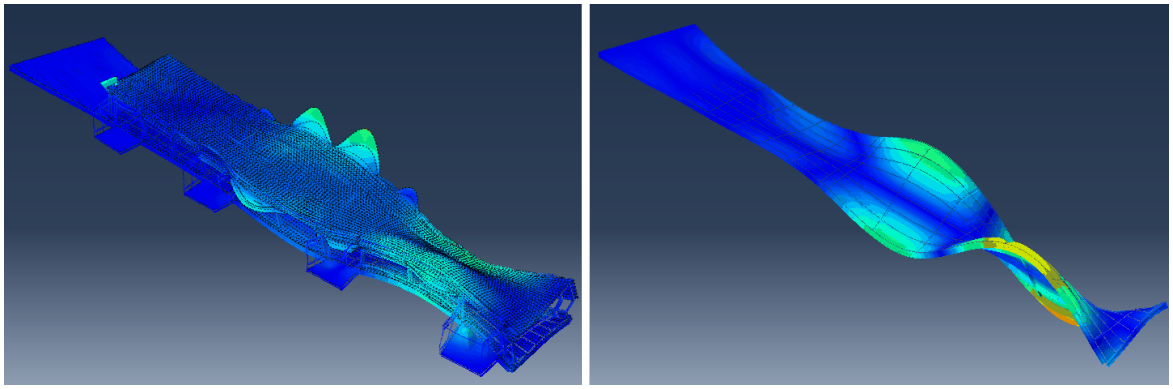

(b) Mode 21 found at 7.59 Hz.

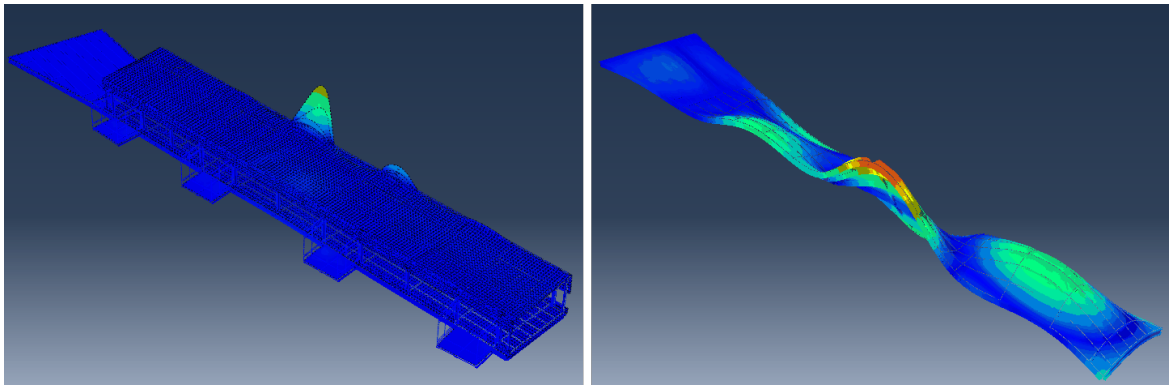

(c) Mode 39 found at 9.15 Hz.

Figure 8.4: Mode shapes corresponding to the first 3 natural frequencies, from the top 5.57, 7.59 and 9.15 Hz, triggering resonance in the deck of Model 1.

8.1.2 Model 2 - HEA400

Changing profiles of the HEA-beams resulted in a decrease of up to 15% of the first natural frequencies compared to **Model 1** as shown in Table 8.2. Natural frequencies of **Model 2**, triggering resonance in the deck are found at 4.73 and 7.07 Hz in the FRF of Figure 8.5 with corresponding mode shape as in Figure 8.4 of **Model 1**.

Table 8.2: Resonance frequencies of Model 1 and Model 2.

Model 1		**Model 2**		
Mode Nr.	**Freq.** [Hz]	**Mode Nr.**	**Freq.** [Hz]	**Dev.**
6	5.57	4	4.73	-15 %
21	7.59	19	7.07	-7 %

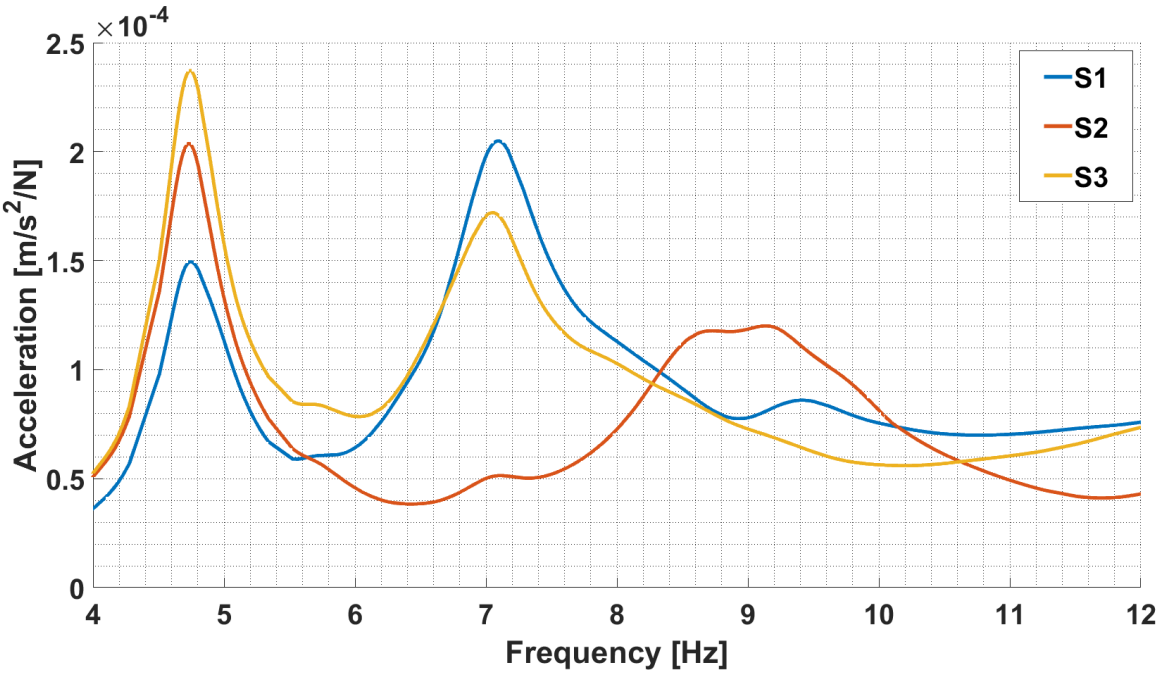

Figure 8.5: FRF of point S1-S3 in Model 2 from mean value of exciting point E1-E7.

8.1.3 Model 3 - Reduced model

Removing the corrugated steel in **Model 3** have a evident effect on the dynamic response, resulting in a decrease up to 23% of the first natural frequencies compared to **Model 1**, shown in Table 8.3. The first natural frequency is found at 4.28 Hz with a new mode shape shown in Figure 8.7. The second mode at 5.02 Hz have the same mode shape as mode 6 in Figure 8.4a.

Table 8.3: Natural frequencies, triggering resonance in the deck, between Model 1 and Model 3.

Model 1		**Model 3**		
Mode Nr.	**Freq.** [Hz]	**Mode Nr.**	**Freq.** [Hz]	**Dev.**
-	-	8	4.28	-23%
6	5.57	19	5.02	-10 %
21	7.59	40	6.76	-11 %

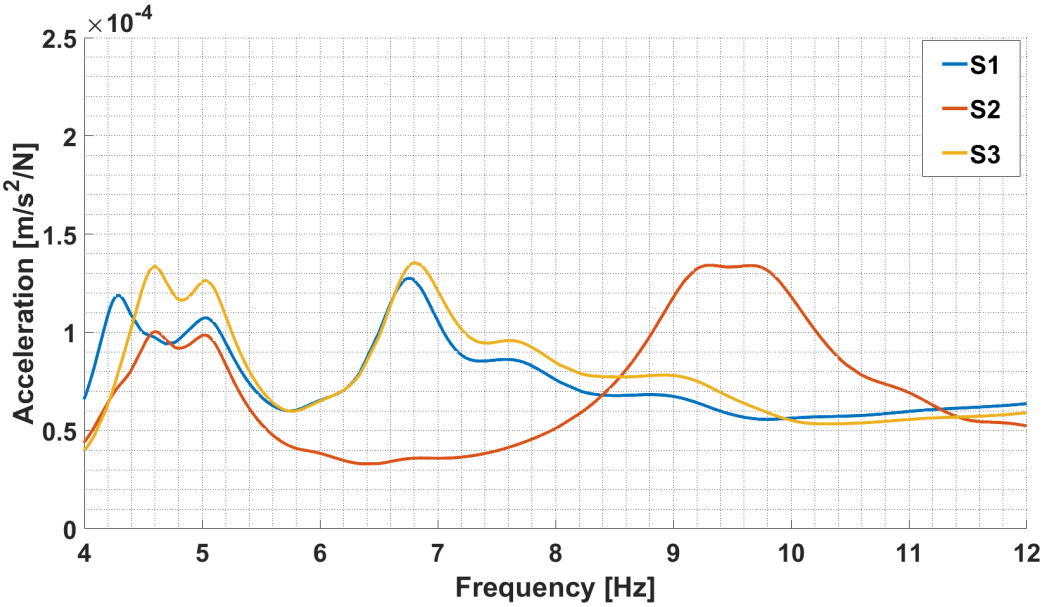

Figure 8.6: FRF of point S1-S3 in Model 3 as mean value of exciting point E1-E7.

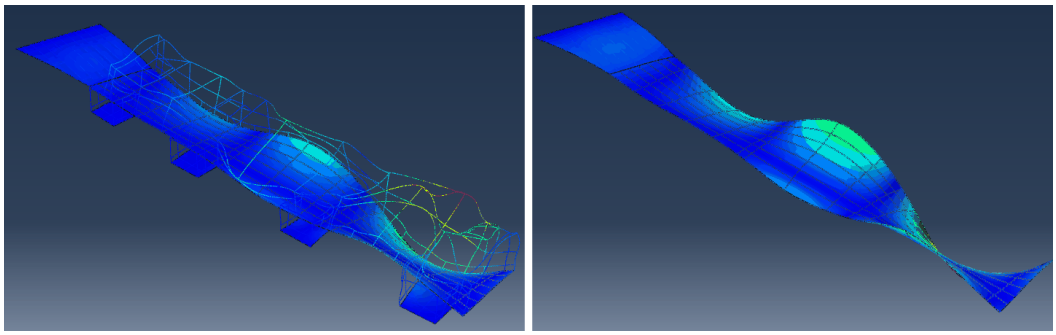

Figure 8.7: Mode shapes corresponding to the first natural frequencies at 4.28 Hz of Model 3.

8.2 Validation - Model 1

To validate the FE-model the FRF of **Model 1** is compared to corresponding measurements of the constructed bridge in Chapter 6, where each point S1-S3 are plotted individually to highlight similarities.

It is shown in Figure 8.8 that FRF of the FE-model matches the field measurements well, especially for the first two modes, 6 and 21 where the natural frequencies are less than 3% apart and accelerations are within 15-26%.

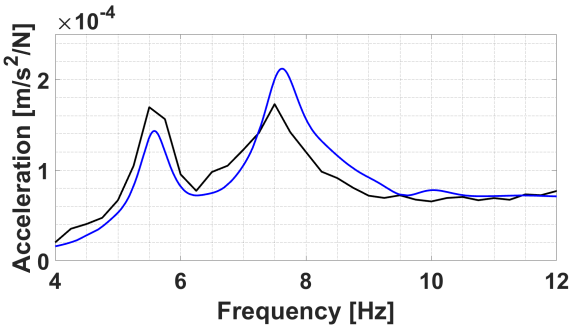

(a) Point S1. See legend in c).

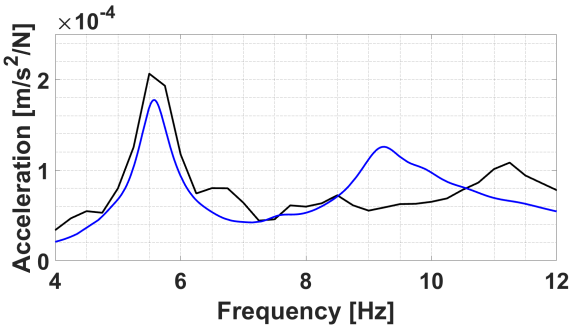

(b) Point S2. See legend in c).

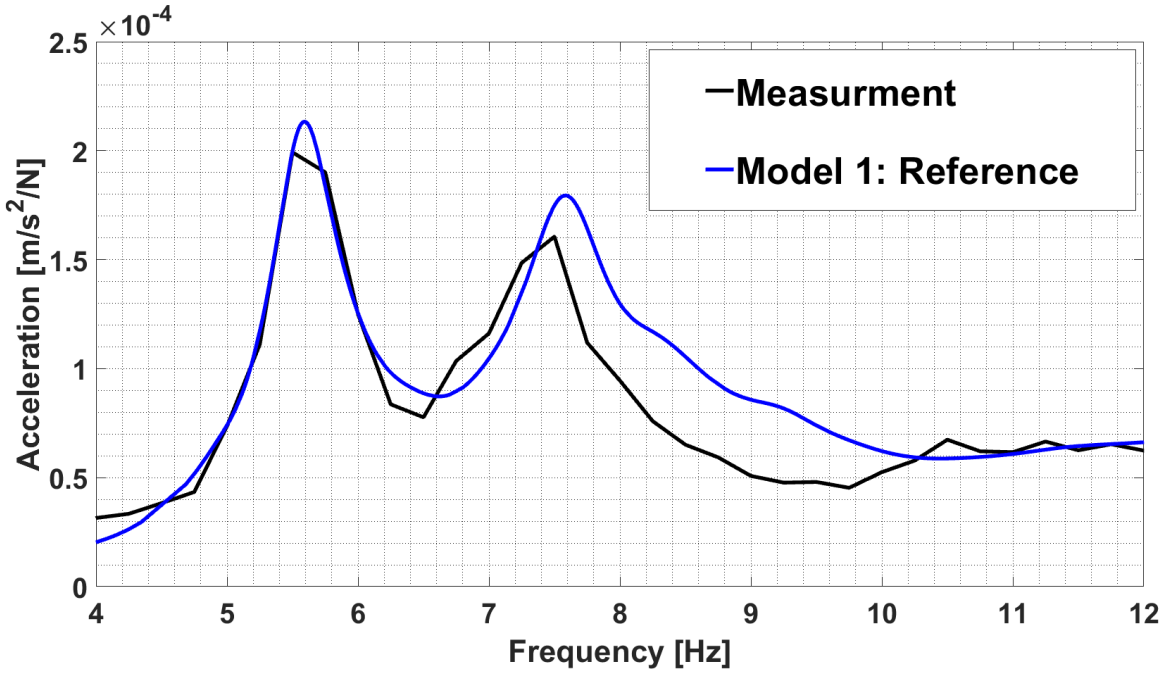

(c) Point S3.

Figure 8.8: FRF compared between Model 1 and measurements shown for point S1-S3.

8.3 Model Comparison

The effects on the dynamic response due to changes in the FE-model of **Model 2** and **Model 3** is evaluated by comparing natural frequencies, FRF and comfort class according to Sétra with the reference model, **Model 1**.

8.3.1 Frequency Response Function

The FRF's are compared in Figure 8.9 highlighting the reduced natural frequencies and accelerations of **Model 2** and **Model 3**. The third mode shown in Figure 8.8c, a bending mode primary triggering a response in the middle of the deck, found around 9 Hz is less affected by changes in **Model 2** and **Model 3** compared to the two first modes shown in Figure 8.9b.

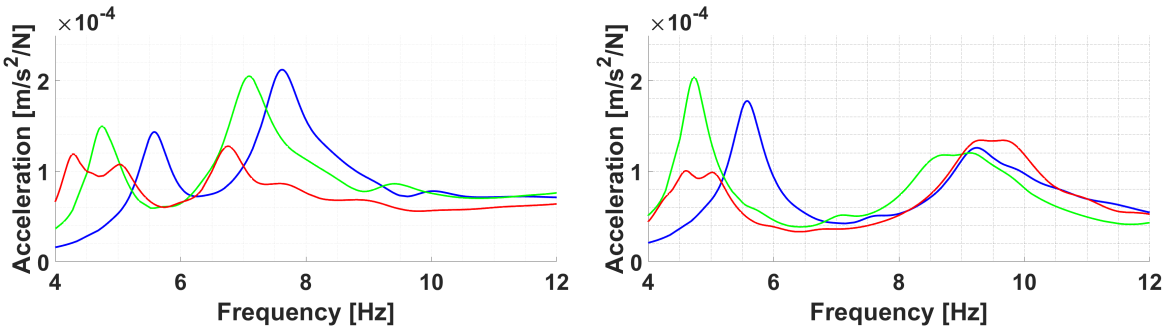

(a) Point S1. See legend in c).

(b) Point S2. See legend in c).

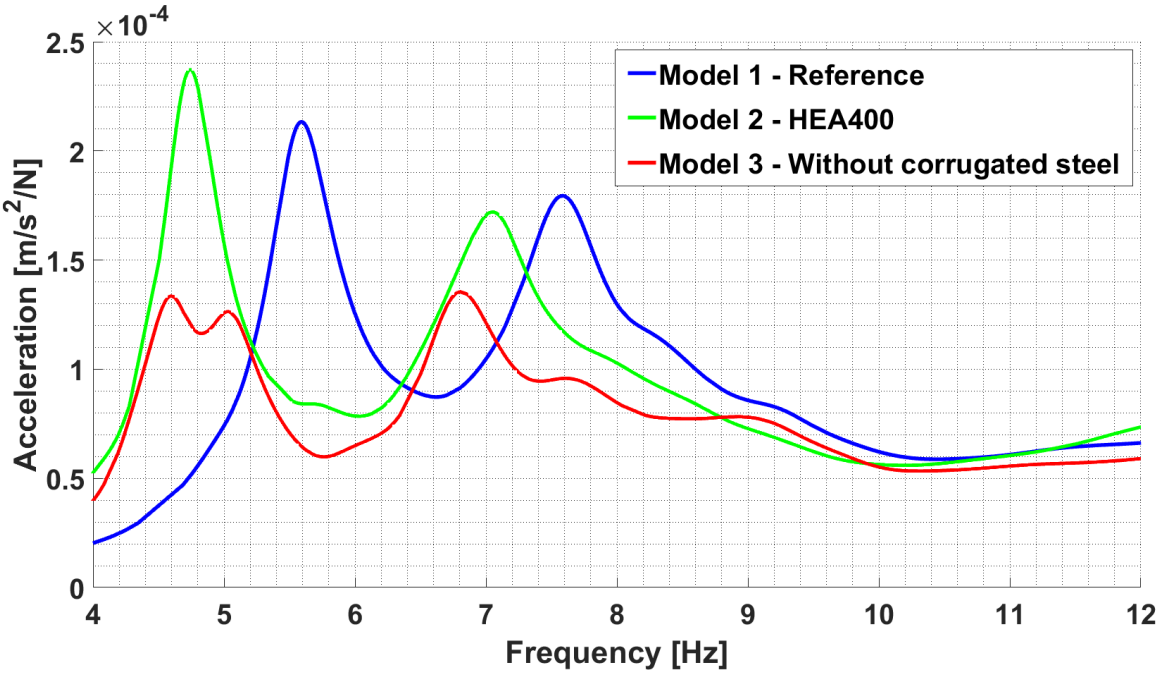

(c) Point S3.

Figure 8.9: FRF of model 1-3 presented for each point S1-S3.

8.3.2 Eigenvalue analysis

The dynamic analysis in Chapter 3.3 shows that natural frequencies are reduced for both models, where **Model 3** is effected the most with a reduction of 23% compared to 15% in **Model 2**.

Mode shapes are unchanged for **Model 2** while the first natural frequency in **Model 3** have a new mode shape shown in Figure 8.7 in Chapter 8.1.3. Mode shape of the second mode in **Model 3** correspond to the first of **Model 1** and **Model 2** in Figure 8.4a.

8.3.3 Comfort class - Sétra

1. Traffic assesment
Skyttelbron is categorized as Class I with a crowd density of 1 person/m^2.

2. Natural frequencies
Natural frequencies are found in the dynamic analysis of Chapter 8.1.

3. Resonance Risk
Natural frequencies places each model in respective risk range.
Model 1 Range 4; negligible risk for resonance
Model 2 Range 3; low risk of resonance
Model 3 Range 3; low risk of resonance

4. Dynamic load-case
Relevant load cases are determined based resonance risk and bridge class, applied according to the mode shape of the first natural frequency, shown in Figure 8.10.
Model 1 No further calculations required
Model 2 load case 2 Eq. 4.3 $p_0 = 5.77$ $\psi = 0.68$
Model 3 load case 2 Eq. 4.3 $p_0 = 5.77$ $\psi = 0.98$

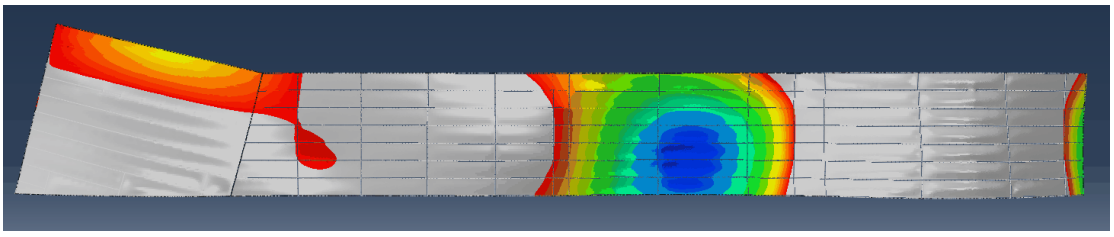

(a) Loading according to mode shape corresponding to mode 6 in Figure 8.4.

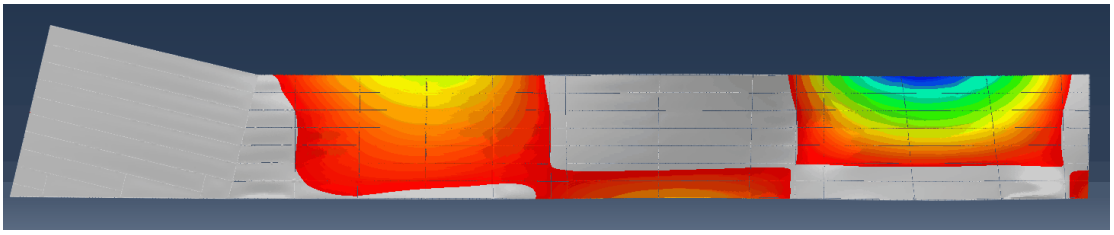

(b) Mode shape corresponding to mode in Figure 8.7

Figure 8.10: Loading in form of the first mode shapes for Model 1 and Model 2 in a) and Model 3 in b).

5. Calculation of accelerations
Peak accelerations are calculated by a frequency sweep, for all load frequencies f_i in Equation 4.3, and the interval 0-15 Hz using SSD; modal analysis with 1% modal damping.

Peak acceleration for point S1-S3 are presented in Table 8.4 with FRF of point S3 displaying maximum acceleration of all models in Figure 8.11. Final accelerations and comfort level is presented in Table 8.5

Table 8.4: Normalized peak accelerations in point S1-S3 for respective model, extracted from corresponding FRF.

Model	**S1** [m/s^2]	**S2** [m/ s^2]	**S3** [m/ s^2]
Full model	0.0870	0.1121	0.1345
HEA400	0.0903	0.1344	0.1526
Reduced	0.0187	0.0167	0.0218

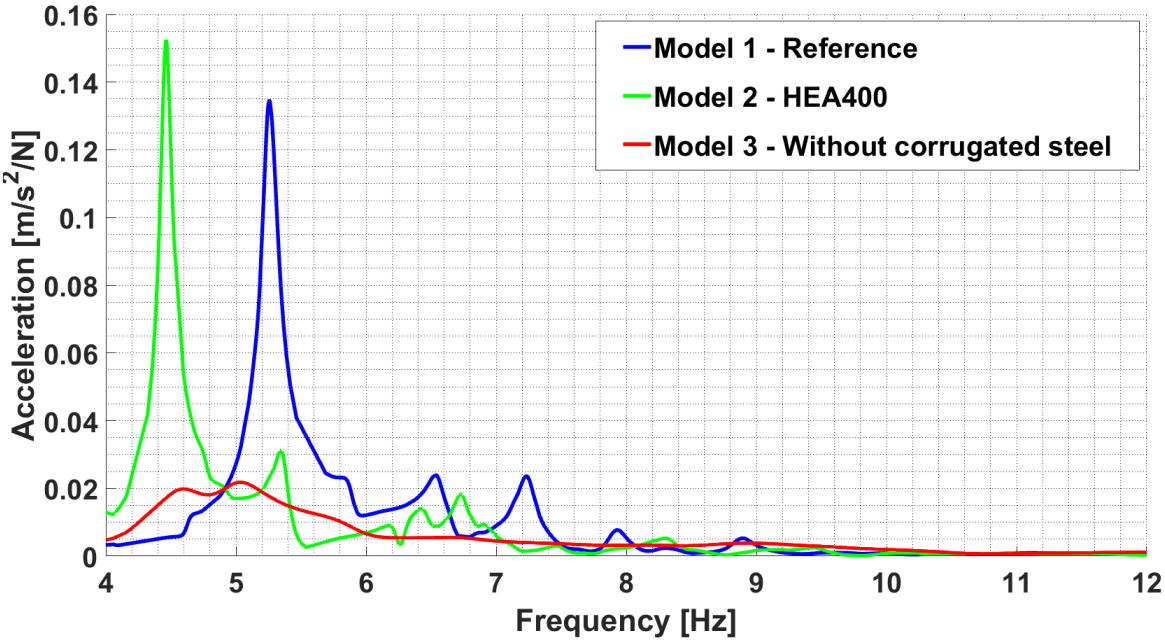

Figure 8.11: FRF of point S3 with loading according to first natural frequency. Peak acceleration, of point S3 above, is presented in Table 8.4for each model.

Table 8.5: Result from the Sétra evaluation of comfort levles.

Model	**Freq.** [Hz]	**Acc.** [m/s^2]	p_0	ψ	**Fin. Acc.** [m/s^2]	**Comfort Class**
Reference	5.25	0.135	-	0	0	1
HEA400	4.46	0.153	5.77	0.68	0.60	2
Reduced model	4.22	0.009	5.77	0.98	0.05	1

8.4 Parametric study

The parametric study is divided in to two main parts investigating how the dynamic response is affected by different ways of modelling stiffness and mass. The study is conducted by gradually altering parameters individually in **Model 1** and comparing the response to the reference model. An overview of investigated parameters are presented in Table 7.5.

8.4.1 Stiffness

Stiffness is studied for the corrugated steel, deck and intermediate beams. The stiffness is changed by altering thickness of the material while compensating the density to keep the mass intact for the corrugated steel and deck. Stiffness of intermediate beams are changed by altering the joints and E-module.

Corrugated steel

The dynamic response is evaluated for thicknesses 1, 2 and 5 mm of the corrugated steel, where 1 mm correspond to the reference model, **Model 1**. The FRF's are compared in Figure 8.4.1 also including the FRF of **Model 3**, completely removing the corrugated steel.

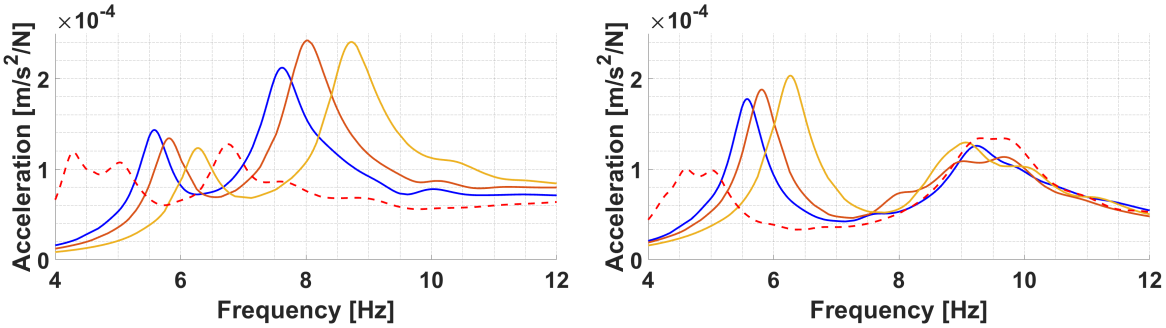

(a) Point S1. See legend in c).

(b) point S2. See legend in c).

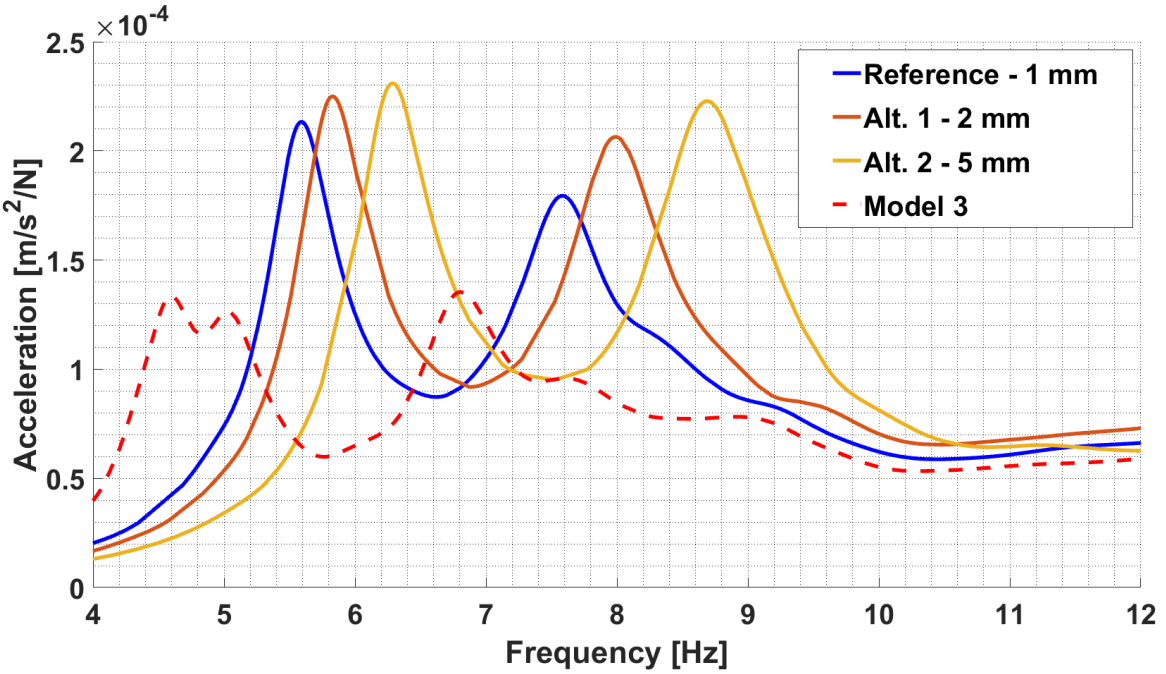

(c) Point S3.

Figure 8.12: FRF for increasing stiffness of the corrugated steel in Model 1, point S1-S3.

Deck

The dynamic response is evaluated for thicknesses 10, 15 and 25 mm of the deck, where 10 mm correspond to the reference model, **Model 1**. The FRF's are compared in Figure 8.4.1.

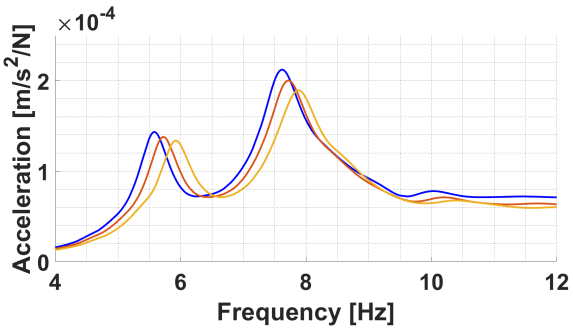

(a) Point S1. See legend in c).

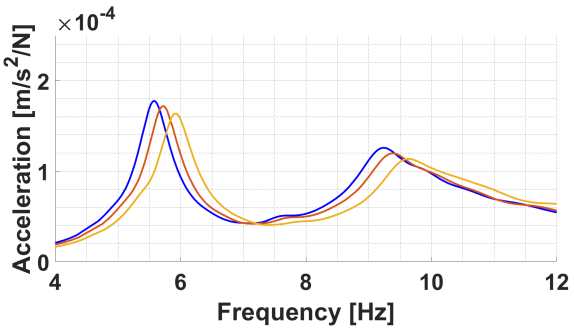

(b) point S2. See legend in c).

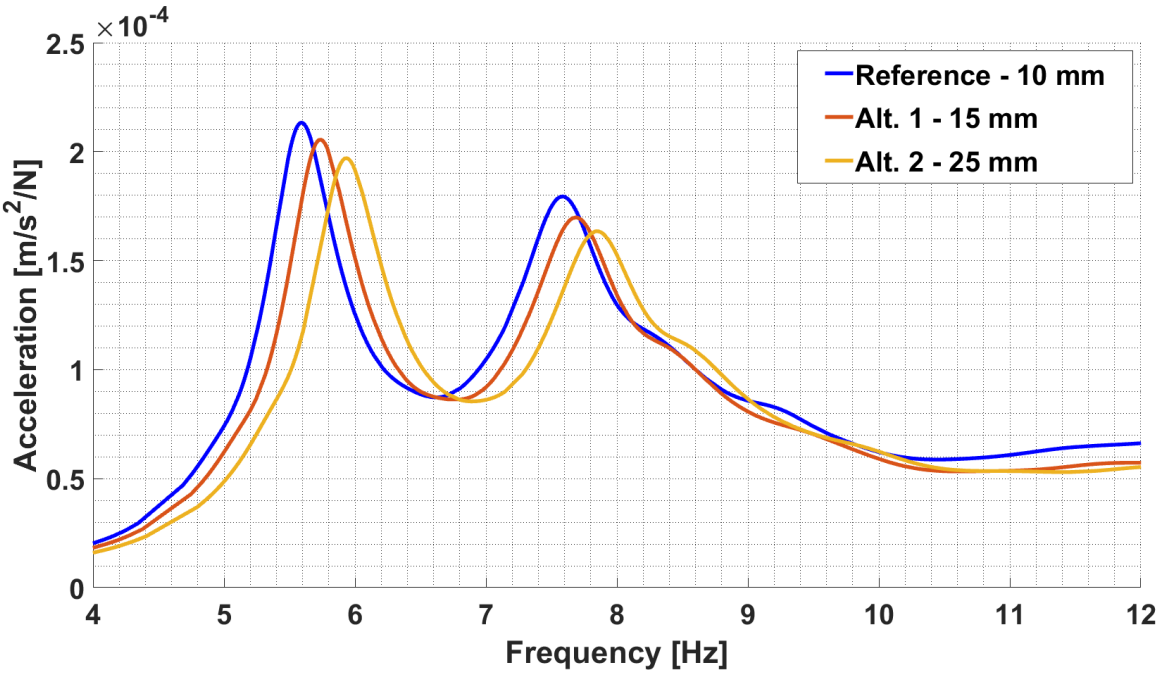

(c) Point S3.

Figure 8.13: FRF for increasing stiffness of the Deck in Model 1, point S1-S3.

Intermediate beam members

The dynamic response is evaluated for free joints, locked joints, and locked joints with increased E-module, where free joints correspond to the reference model, **Model 1**. The FRF's are compared in Figure 8.4.1 also including the FRF completely removing the intermediate beams. Locked and free joints reefers to modeling of rotational dofs in the FE-model.

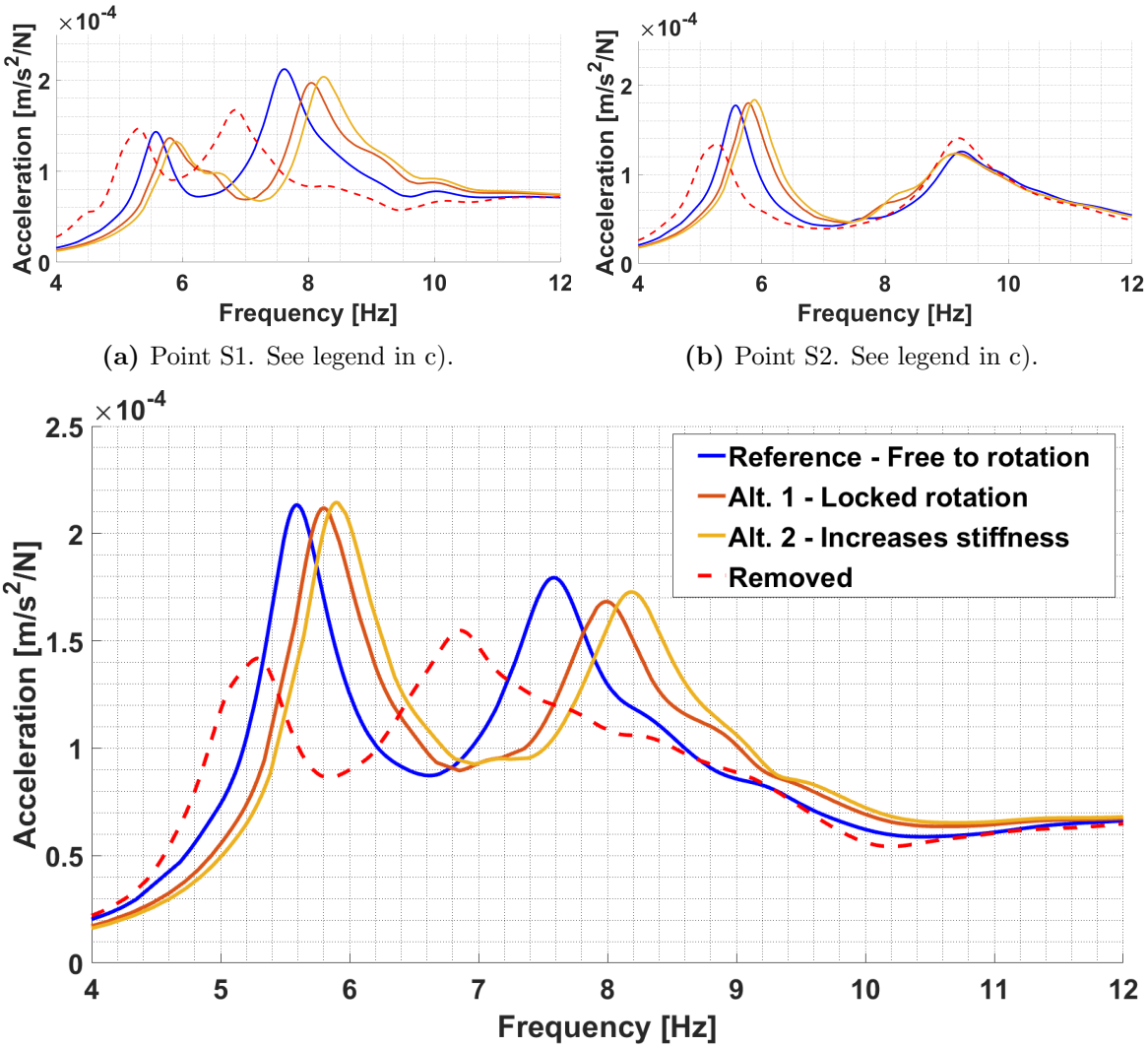

(a) Point S1. See legend in c).

(b) Point S2. See legend in c).

(c) Point S3.

Figure 8.14: FRF for increasing stiffness of the intermediate beams in Model 1, point S1-S3.

8.4.2 Mass

The effect on the dynamic response of the FE-model for different ways of modelling the mass is examined from two perspectives, mass quantity and mass distribution.

Mass - Quantity
The dynamic response is evaluated for an nonstructural mass, representing installations etc., of 45, 68 and 90 tons where 45 tons correspond to the reference model, **Model 1**. The FRF's are compared in Figure 8.4.2 also including the FRF when completely removing the mass.

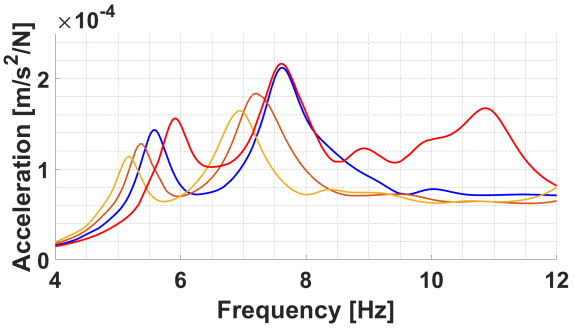

(a) Point S1. See legend in c).

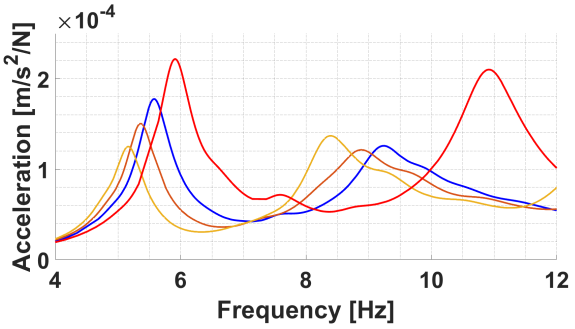

(b) Point S2. See legend in c).

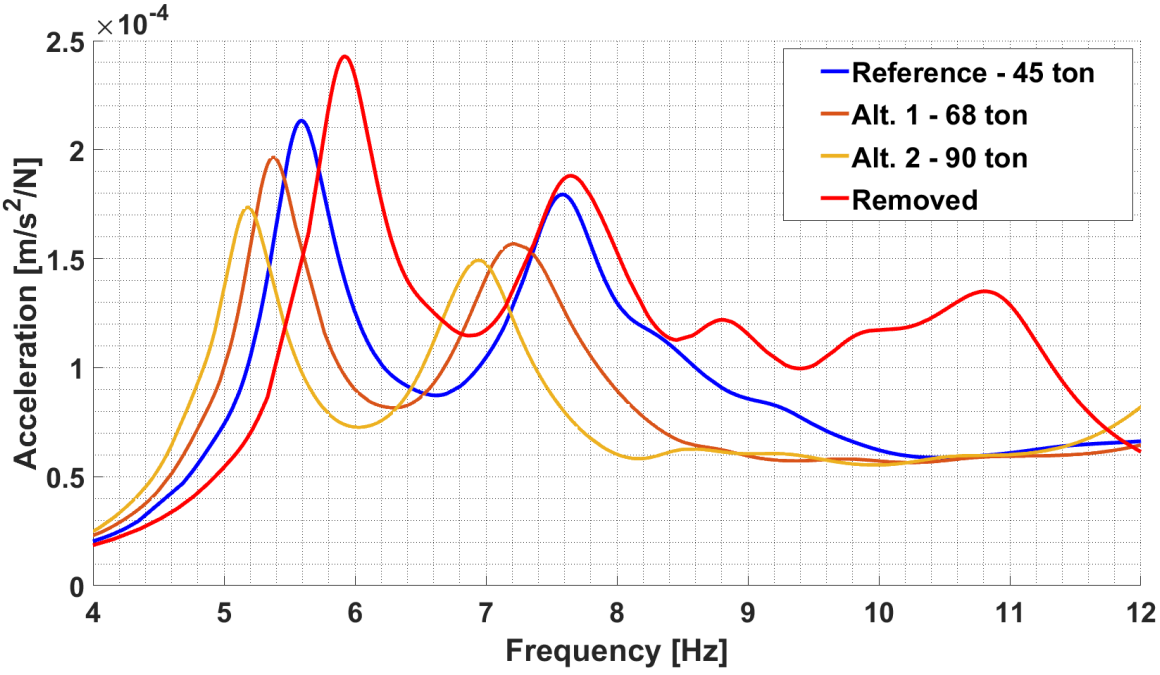

(c) Point S3.

Figure 8.15: FRF when altering quantity of the nonstructural mass in Model 1, point S1-S3.

Mass - Distribution

The dynamic response is evaluated with nonstructural mass placed as a line-load, point-load and uniform-load where the line-load correspond to the reference model, **Model 1** shown Chapter 6 in Figure 7.16. The FRF's are compared in Figure 8.4.2 and twisting mode as a result from mass placed high up, Figure 8.16.

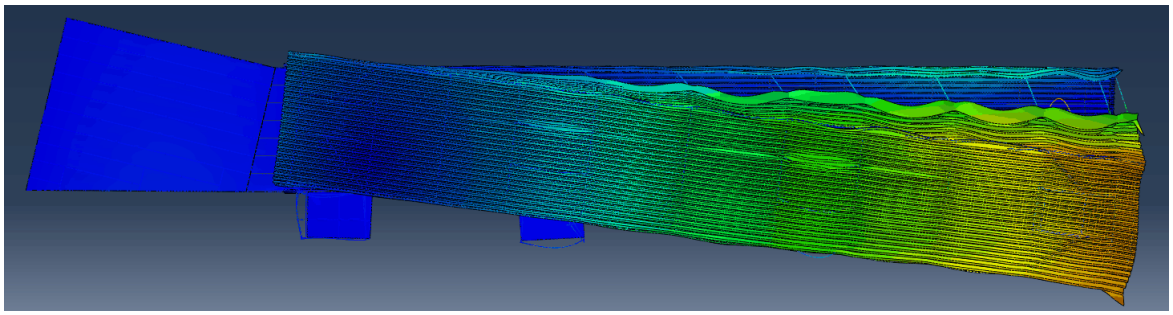

Figure 8.16: Twisting mode obtained only when placing the mass high up in the models.

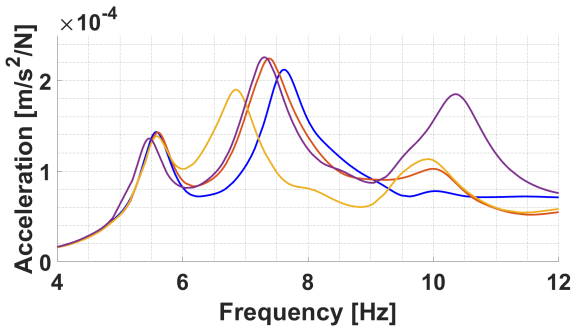

(a) Point S1. See legend in c).

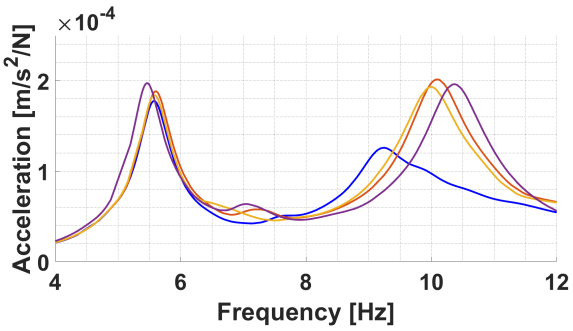

(b) Point S2. See legend in c).

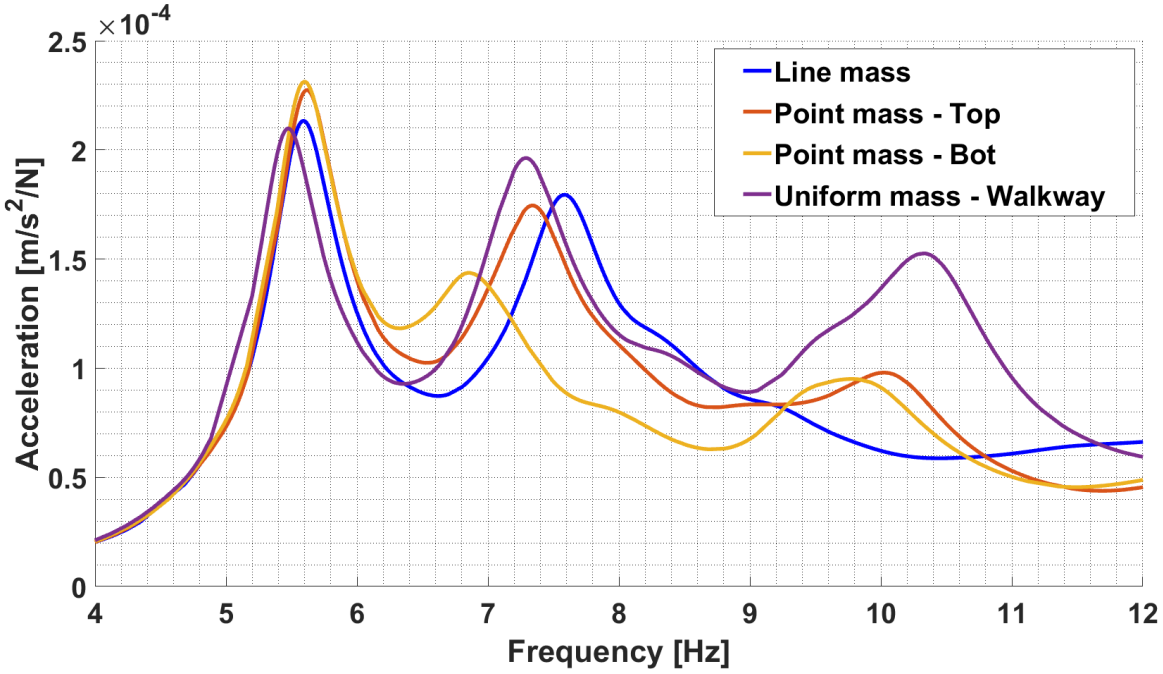

(c) Point S3.

Figure 8.17: FRF when altering placement of the nonstructural mass in Model 1, point S1-S3.

9 Discussion and conclusions

9.1 FE-modelling and validation

A FE-model will always be an idealization of the real structure, containing simplifications and uncertainties to some degree. It is important to keep that in mind when creating the model as it is evident that there is a direct relationship between assumptions made in the model and the model response. Simplifications should only be made if they improve prerequisite in some way without altering the final result too much.

Boundary conditions have been changed gradually in the modeling process as mode shapes were continuously evaluated while more sections of the bridge were added to conclude that boundary conditions does not impact the dynamic response in a negative way. The initial model was first modeled without the ramp and stairwells, sections which were later added as the boundary conditions showed to play a critical role for the dynamic behaviour of the FE-model.

The first complete version of the FE-modeled, containing all structural members, showed a very realistic dynamic response from start, compared to the measurements of the constructed bridge. After the first comparison of the dynamic response, only minor adjustment were made to calibrate natural frequencies and obtain the final state of the reference model, **Model 1**. Natural frequencies were calibrated by increasing total mass by 5% through adjustment of the non-structural mass.

Comparing FRF's as presented in Chapter 8.2 of the reference model and measurements it is evident that both natural frequencies and accelerations are exceptionally close to the measurements, implicating an high credibility of the model. This is further supported when considering how well the FE-model match not just one, but the two first natural frequencies. Great resemblance is also found in the mode shapes of the second mode when comparing the forms in Figure 8.4b and 6.3b.

The FE-model provides excellent result for the purpose of this thesis to compare the dynamic evaluation of different modeling options. But it is necessary to keep in mind that natural frequencies are a result of the mass-stiffness relationship shown in Equation 2.2. This means that even if the relationship between them are accurate, both parameters can be under- or overestimated. When designing a bridge, it is thereby important to estimate the unknown mass accurately and to make qualified assumptions regarding simplifications that may affect the stiffness of the FE-model.

The total mass of the reference model amounts to 322 tons which is not unreasonable, but nonstructural mass representing installations, joints etc. representing that the unknown mass makes up about 20% of the total mass which is more questionable and could be further investigated.

9.2 Discussion on parametric study

All parameters investigated in the parametric study have had an effect to the dynamic response in some extent, but with various importance of the dynamic evaluation.

9.2.1 Influence of stiffness

The parametric study shows that an increased stiffness of the structural members in general raises natural frequencies as can be expected based on the theory in Chapter 2.

It also shows that an increased stiffness of individual members impact mode types differently,implicating that structural design have a direct effect on mode shapes obtained from the analysis. This can be observed in Figures 8.4.1 and 8.4.1 where alternating the stiffness of the corrugated steel and intermediate beams primarily affected effect the twisting modes, the first two modes. It had, how ever, very small or negligible effect on the bending mode, the third mode. This means that individual members may have different importance to the dynamic evaluation depending on the structural design and which mode shapes that are relevant to be evaluated.

Greatest effect on the dynamic response, can be observed by studying the results in the same Figures when comparing the alternatives to include or exclude the parts completely. All cases including the part shows a more realistic dynamic response, compared to when it is excluded. This implicates that it is more important to include relevant elements at all, to account for their stiffness contribution, compared to how precise they are modeled.

9.2.2 Influence of mass

In contrast to the stiffness, increased mass general decreases natural frequencies and accelerations. This is also an expected response based on the theory in Chapter 2. Changing the mass quantity, with analysis results shown in Figure 8.4.2, displays a translation of the whole curve with a relationship that is close to linear compared to the mass change. The same effect was observed during the modeling process for other elements when altering their mass in the same way.

As the effect of change in mass quantity is primarily depending on the absolute change of mass compared to total mass of the bridge it means that altering mass of individual elements will have a relatively small impact on the dynamic response. For example, doubling the mass of the corrugated steel resulted in a total mass increase of only 4% while it is obvious that the weight of the corrugated steel is way overestimated. It is thereby, regarding mass properties of individual parts, more important to include the mass within a realistic interval, compared to how precise it is modeled.

Distribution of mass has shown to have a direct effect on the modes shape of the FE-model. Moving mass from the upper part of the superstructure to the deck have resulted in that twisting modes as shown in Figure 8.16 have disappeared.

It is difficult, from observing the FRFs in Figure 8.4.2 to draw any conclusions on the effect of mass distribution has on the dynamic response of the deck. Most cases provide similar results for the two first modes, with exception for placing the point mass at the bottom.

9.3 Evaluation of Dynamic Response

The eigenvalue analysis performed in a FE-analysis results in a lot of natural frequencies and it can be hard to distinguish which modes that is relevant to evaluate. By combining the results from the eigen value- and FRF in the dynamic analysis in Chapter 8.1 it is shown that both primary and secondary elements have a direct effect on the natural frequencies. The first natural frequency of interest, triggering resonance in the deck, is found at 5.57, 4.72 and 4.28 Hz for each respective model, model 1-3.They are all relatively high frequencies for a lightweight steel pedestrian bridge, where accelerations only need to be evaluated for natural frequencies below 5 Hz, according to Eurocode. In this case only **Model 2** and **Model 3**.

The dynamic analysis of **Model 2** resulted in low vertical accelerations placing it in the lower part of Range 2 with a medium comfort level compiled in Table 8.5. This shows that Skyttelbron could have been designed with HEA400 beam members, reducing the mass of primary load bearing members by over 20%. Provided that an evaluation of acceleration would have been performed according to the Sétra method with a realistic FE-model as used in this case and that medium comfort level is acceptable.

Modeling Skyttelbron completely without the corrugated steel is shown to affect the dynamic evaluation negative as natural frequencies are decreased, forcing an evaluation of accelerations on the unsafe side. Because of the high natural frequencies of the bridge this did not affect the final outcome of the comfort class according to Sétra.

That accelerations dropped when the stiffness of the corrugated steel were decreased or removed, shown in Figure 8.13 was not an expected result. One suggestion to explain this result could be that when individual parts of the upper structure is restrained from moving freely, by the corrugated steel, they will instead move in synchronization creating a twisting mode that also affects the deck.

9.4 Conclusions

- The results of the FE-model shows good correlation with the dynamic response of the constructed bridge as measured and provide sufficient results for the purpose of this thesis.
- The mass of load bearing member could been reduced by over 20% by evaluating acceleration according to Sétra with a realistic FE-model.
- Secondary elements should be included in the FE-model as they have an evident effect on the dynamic behaviour.
- The effect on the dynamic response when including secondary members in a FE-model depends on the overall structural design and specific points of interest.
- It is in general more important to include all elements rather than how precise they are modeled.
- Boundary conditions play a critical role for the dynamic behaviour from the FE-model.
- Unknown mass of the bridge is one of the greatest uncertainties affecting the results from FE-model during the design phase.
- Increased stiffness in general raises natural frequencies.
- Increased mass in general decreases natural frequencies and reduces accelerations.
- The damping of the first modes of the constructed bridge was from the measurements found to be very high.

9.4.1 Mini Guide to Dynamic Analysis:

Creating the FE-model

- **Boundary conditions:** plays a critical role in the dynamic response of the FE-model. Make sure to model supports corresponding to real conditions. For larger structures make sure to include relevant sections and choose boundary conditions against secondary structures carefully. The boundary conditions against secondary structure should either be very obvious or placed further away from the point of interest.
- **Secondary elements:** it is more important to include relevant elements than how precise they are modeled.
- **Choosing members:** Consider probable mode shapes of the structure and how individual members would affect the response. Ex. if a twisting mode effect the point of interest, what elements effects the twisting.
- **Mass quantity:** should be carefully estimated as it is one of the greatest uncertainties in the FE-model and can have major effect on the dynamic evaluation.
- **Mass distribution:** should strive to have a realistic distribution as it affect which mode shapes and can have a major effect on the dynamic evaluation.

Determine if risk for resonance

- **Obtain all natural frequencies** below 5 Hz through an eigenvalue analysis.
- **Single out relevant modes** from an FRF showing natural frequencies triggering resonance in the points of interest.

Evaluate acceleration of frequencies below 5 Hz according to the Sétra method.

Determine bridge class and comfort criteria.

Recalculate eigen frequencies with increased load, 70 kg/m^2

Obtain accelerations from the FRF with load applied in respective mode shape corresponding to natural frequencies of interest.

Determine load case and calculate load- and reduction factor.

Calculate final acceleration and evaluate against chosen comfort criteria.

If accelerations is not acceptable, consider possible solutions suggested in Eurocode.

9.5 Future work

- investigate how to efficiently improve the dynamic response by change in the bridge structure. For example alternative ways of designing supports, intermediate elements and mass properties.
- Further investigate damping of constructed bridge and how it is considered in current design criteria.
- Determine how displacement amplitude is affected by mass and stiffness properties in correlation to the frequency and acceleration response of the FE-model.

Bibliography

[1] *SS-EN 1990*. SIS Förlag AB, 2002-06-28.

[2] *Footbridges Assessment of vibrational behaviour of footbridges under pedestrian loading*. Service d'etudes techniques des routes et autoroutes - Setra, 2006.

[3] João R. Correia Luís Guerreiro Augusto M. Gomes Mário F. Sá Nuno Silvestre. *Dynamic behaviour of a GFRP-steel hybrid pedestrian bridge in serviceability conditions. Part 2: Numerical and analytical study*. Elsevier Ltd., 2017.

[4] Anil K. Chopra. *Dynamics of Structures, Fifth Edition*. Pearson Education Limited, 2017. ISBN: 978-1-29-224918-6.

[5] Hans Petersson Niels Saabye Ottosen. *Introduction to the Finite Element Method*. Pearson Education Limited, 1992. ISBN: 978-0-13-473877-2.

[6] Dassault Systémes Simulia Corp. *Abaqus/CAE*. Version 2019.

[7] Trafikverket. *Konstruktionsritningar Skyttelbron*. AFRY AB, 2014.

[8] Ruukki Sverige AB. *Load-bearing profiled sheet Installation instructions*. URL: https://www.ruukki.com/docs/default-source/b2b-documents/load-bearing-sheets/load-bearing-sheets/ruukki-load-bearing-profiled-sheet-installation-instructions.pdf?sfvrsn=13637269725930800000 (visited on 23/04/2022).

[9] Brüel Kjær. *Brüel Kjær Sound and Vibration measurement*. URL: https://www.bksv.com/en (visited on 23/04/2022).